Chapter 15
Computational Models of Auxin-Driven Development

Adam Runions, Richard S. Smith, and Przemyslaw Prusinkiewicz

Abstract Auxin plays a key regulatory role in plant development. According to our current understanding, the morphogenetic action of auxin relies on its polar transport and the feedback between this transport and the localization of auxin transporters. Computational models complement experimental data in studies of auxin-driven development: they help understand the self-organizing aspects of auxin patterning, reveal whether hypothetical mechanisms inferred from experiments are plausible, and highlight differences between competing hypotheses that can be used to direct further experimental studies. In this chapter we present the state of the art in the computational modeling of auxin patterning and auxin-driven development in plants. We first discuss the methodological foundations of model construction: computational representations of tissues, cells, and molecular components of the studied systems. On this basis, we present mathematical models of auxin transport and the essential properties of pattern formation mechanisms involving auxin. We then review some of the key areas that have been investigated with the use of models: phyllotactic patterning of lateral organs in the shoot apical meristem, determination of leaf shape and vasculature, long-distance signaling and apical control of development, and auxin patterning in the root. The chapter is concluded with a brief review of current open problems.

A. Runions • P. Prusinkiewicz (✉)
Department of Computer Science, University of Calgary, Calgary, AB, Canada
e-mail: pwp@cpsc.ucalgary.ca

R.S. Smith
Department of Comparative Development and Genetics, Max Planck Institute for Plant Breeding Research, Cologne, Germany

1   Introduction

A key objective of developmental biology is to understand how molecular processes drive the development of tissues, organs, and entire organisms. In plants, the growth regulator auxin plays a commanding role on which many developmental processes depend. The morphogenetic role of auxin begins in the embryo, where its dynamic, differential distribution establishes the shoot–root polarity (Weijers and Jürgens 2005). In post-embryonic development, diverse patterning, signaling, and regulatory functions of auxin are summarized by the reverse/inverse fountain model (Benková et al. 2003) (Fig. 15.1). According to this model, auxin is produced in the vicinity of the shoot apical meristem and is transported in the epidermis towards the peripheral zone of the apex. There it accumulates in emergent convergence points, which determine the phyllotactic pattern of the incipient plant organs: leaves, flowers, and new branches (Reinhardt et al. 2003; Jönsson et al. 2006; Smith et al. 2006a). As a leaf grows and becomes flat, further convergence points appear at the leaf margin (Scarpella et al. 2006; Hay et al. 2006). These points may be correlated with the growth pattern localized near the margin, leading to the formation of serrated (Hay et al. 2006; Bilsborough et al. 2011), lobed, or compound (Barkoulas et al. 2008; Koenig et al. 2009; Ben-Gera et al. 2012; Townsley and Sinha 2012) leaves. From the primordia auxin flows into the subepidermal layers of the apex and, subsequently, into the plant stem. In this process, it is "canalized" into narrow paths (Sachs 1969, 1991; Mitchison 1980, 1981; Rolland-Lagan and Prusinkiewicz 2005; Feugier et al. 2005; Bayer et al. 2009; O'Connor et al. 2014), which, in the case of a leaf, mark the location of the primary vein and its extension into stem vasculature. Within the stem, auxin is involved in the patterning of the vascular system and the activation of lateral buds (Bennett et al. 2006; Prusinkiewicz et al. 2009; Crawford et al. 2010), thus coordinating the development of the branching plant structure (Leyser 2011). From the stem, auxin continues on to the root system, flowing through the root–shoot transition zone towards the apical meristems of the main and lateral roots, and reversing its direction in the root epidermis. In this process, it is involved in the maintenance and growth of sharply bounded meristematic and elongation zones (Grieneisen et al. 2007), initiation of lateral rootlets (Benková et al. 2003; Laskowski et al. 2008; Lucas et al. 2008a, b; Moreno-Risueno et al. 2010), and tropic responses to gravity (Swarup et al. 2005; Zažímalová et al. 2010).

The ability of auxin to perform these diverse functions is related to the pattern of its transport and the feedback between transport and the intercellular distribution of transporters. This includes, in particular, the highly mobile efflux carriers from the PIN protein family. In recent years, the interplay between auxin and further morphogenetic factors, such as other hormones, nutrients, light, and mechanical forces acting on cells, has also been considered (Leyser 2009). Computational models play a significant role in the studies of auxin-related patterning. The importance of these models stems from the self-organization of the patterning processes. Causal links underlying the emergence of patterns through self-

Fig. 15.1 Processes and patterns regulated by auxin in post-embryonic development according to the reverse (shoot) and inverse (root) fountain model (Benková et al. 2003). *Blue arrows* indicate the paths and directions of auxin flow. *Blue circles* mark points of auxin accumulation. From (Prusinkiewicz and Runions 2012)
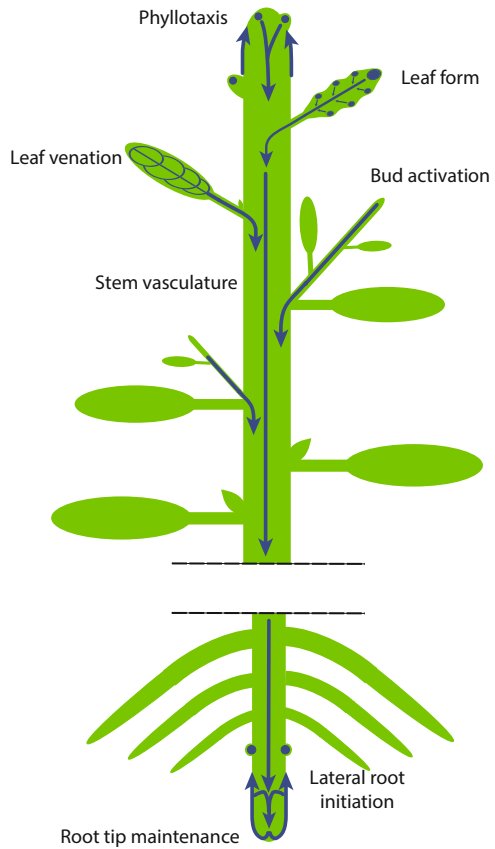
organization are generally nonintuitive, and computational models are a valuable tool facilitating their understanding (Camazine et al. 2001; Prusinkiewicz and Runions 2012). Models of auxin-driven patterning range from those directly rooted in biochemistry (Renton et al. 2012; Steinacher et al. 2012; Hošek et al. 2012) to more abstract constructs that aim at deducing morphogenetic characteristics of molecular-level process from the observed patterns and forms. In some cases, several hypotheses have been proposed to explain the same phenomenon, for example, the formation of phyllotactic and vascular patterns (Merks et al. 2007; Stoma et al. 2008; Bayer et al. 2009). While there is no consensus which of these hypotheses, if any, is the right one, the alternative models highlight their logical consequences and help formulate experiments that may support or falsify each hypothesis. Eventually, the models that survive the test of experiments will establish a causal chain linking molecular processes to macroscopic patterns and forms (Fig. 15.2).

The survey presented in this chapter begins with an outline of computational representations of tissues, cells, and cell states used in models of auxin-driven development. This is a fundamental aspect of model construction, as different
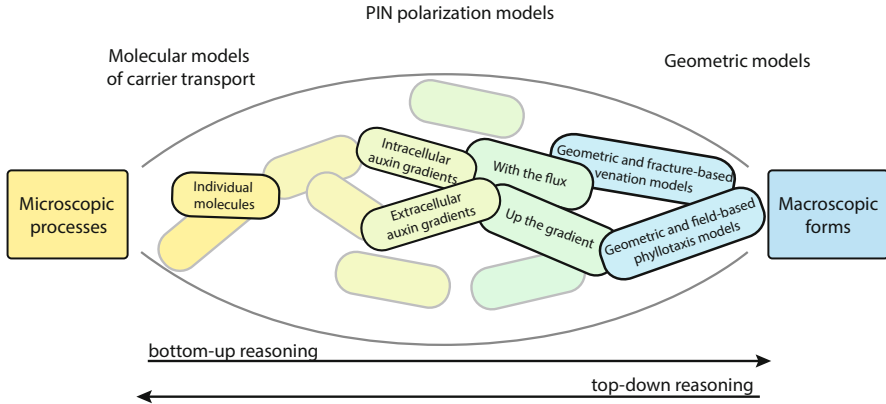
Fig. 15.2 Models formulated at different scales and levels of abstraction represent a partial view of the causal chain that links molecular-level patterning and macroscopic forms

representations reflect different assumptions concerning the modeled processes. Models of auxin transport and polarization of transporters in cells are presented next, followed by a discussion of fundamental patterning properties of the postulated feedback loops (e.g., capability of forming a pattern of peaks or canals of auxin transport). Finally, the reverse/inverse fountain model is used to organize a review of specific models of auxin-driven patterning and plant development. Parts of this survey are an updated version of an earlier work by Prusinkiewicz and Runions (2012).

2   Computational Representations of Cells and Tissues

The choice of computational representations (data structures) of the modeled phenomena affects the range of processes that can be captured by the model, the level of abstraction at which they will be considered, the ease of creating, modifying, and exploring the model, and the computational efficiency of simulations. In the case of auxin-driven patterning, the central question is the relation between processes taking place in individual cells and the patterns emerging at the level of tissues. Consequently, the data structures typically consist of an explicit representation of cells connected into a tissue. Within this general framework, a number of choices exist and have been incorporated into different models.
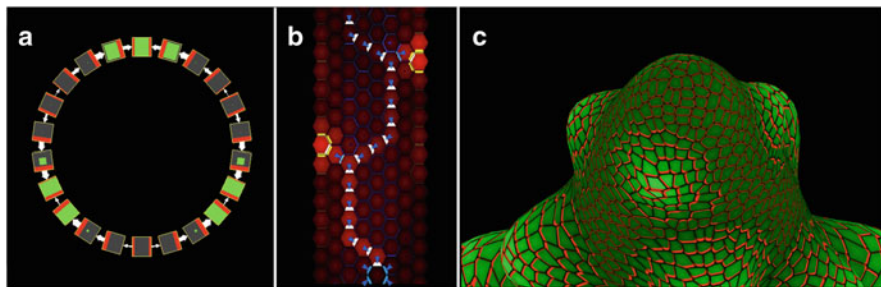
Fig. 15.3 Some tissue representations used in cellular-level models of auxin-driven development. (**a**) One-dimensional ring representing the peripheral zone of a shoot apical meristem patterning the position of three primordia. The model assumes up-the-gradient polarization as described in Sect. 4.1 (Jönsson et al. 2006; Smith et al. 2006a). Auxin concentration in each cell is indicated by the size of the *green square*, PIN localization by the width of *red bars*, and auxin fluxes by the *white arrows* between cells. (**b**) Hexagonal tissue representing a longitudinal section through the shoot of *Brachypodium distachyon*. The model captures phyllotaxis and vascular development as described in Sect. 5.3 (O'Connor et al. 2014). Auxin concentration is shown in *red* and the localization of different PIN types in *yellow*, *blue*, and *white*. (**c**) A polygonal mesh representing the surface of a shoot apical meristem during a simulation of spiral phyllotaxis described in Sect. 5.1 (Smith et al. 2006a). Auxin concentration is shown in *green* and PIN in cell membranes in *red*

2.1 Dimensionality of the Model

Selected basic aspects of patterning, for example, the emergence of auxin concentration peaks (Smith et al. 2006a; Jönsson et al. 2006) or uniformly polarized cell files (Abley et al. 2013), can be explored in one-dimensional models: a sequence, ring (Fig. 15.3a), or branching arrangement of cells. One-dimensional models can be specified, implemented, and analyzed more easily than two- or three-dimensional models, but the scope of phenomena that they can capture is limited. In particular, canalization, i.e., the consolidation of auxin transport into narrow channels that pattern vascular tissues, can only be considered in two or three dimensions.

Two-dimensional models that abstract cells as polygons and cell walls as polygon edges are widely used as a compromise between the limited expressive power of one-dimensional models and the complexity of creating and visualizing fully three-dimensional models. The use of two-dimensional models is often further justified by the nature of the studied processes. For example, phyllotactic patterning in the apical shoot meristem of Arabidopsis is assumed to take place in the single layer of epidermal cells (Reinhardt et al. 2003; Barbier de Reuille et al. 2006; Jönsson et al. 2006; Smith et al. 2006a; Stoma et al. 2008; Kierzkowski et al. 2013), although subepidermal tissues may also play a role (Larson 1975; Banasiak 2011). Patterning of leaf veins is essentially a two-dimensional process. The radial symmetry of roots suggests that modeling a longitudinal root section may suffice to capture the essential features of root morphogenesis (Grieneisen et al. 2007). Even

processes that break this radial symmetry can be modeled in two dimensions if an appropriate section plane is chosen. For instance, the impact of root bending on the distribution of auxin and initiation of lateral roots was successfully modeled in two dimensions (Laskowski et al. 2008). Fully three-dimensional models still present a technical challenge.

2.2 Representation of Cells and Tissues

The simplest two-dimensional models are constructed assuming identical, square (Mitchison 1981; Rolland-Lagan and Prusinkiewicz 2005), or hexagonal (Feugier et al. 2005; Stoma et al. 2008; O'Connor et al. 2014) cells (Fig. 15.3b) . These cells are arranged in a regular tiling pattern, allowing for a straightforward and computationally efficient representation of the tissue as an array of cells. Artifacts of the regular tilings include directional bias (for example, a tissue made of square cells has different properties in the horizontal and vertical directions than in the diagonal directions) and a limited capacity for simulating growth: divisions of internal cells would break the regularity of the tiling, and thus new cells can only be added at the tissue boundary.

In more realistic models, tissues are represented by two-dimensional assemblies of polygons resembling the shape of cells, which form polygon meshes. For example, positions of cell walls and vertices at which they meet may be specified explicitly (Fig. 15.3c), inferred from the position of cell centroids through the construction of a Voronoi diagram, or result from a physically based simulation (see Prusinkiewicz and Runions (2012) for a review and Shapiro et al. (2013) for the most recent result). Diverse computational representations of polygon meshes are possible and have been widely studied due to their importance to geometric modeling and computer graphics. In particular, the vertex–vertex data structure (Smith et al. 2004; Smith 2006), rooted in the mathematical formalism of graph rotation systems (Edmonds 1960; White 1973), has been used in several models of auxin-driven patterning (Smith et al. 2006a; Bayer et al. 2009; Chitwood et al. 2012; Abley et al. 2013; O'Connor et al. 2014). This is due, in part, to the relatively simple specification of tissue growth and cell divisions in this formalism. The model of cell division by Besson and Dumais (2011) highlights the need for representing cells with curved walls, which likely will be incorporated into future models of auxin-driven morphogenesis. Models of jigsaw-shaped pavement cells in leaf epidermis will require even more flexibility in representing cell geometry.

In the above representations, cells typically partition the tissue without gaps or overlaps (except for the shared walls). Accumulation and diffusion of auxin in the intercellular space is neglected, and auxin leaving a cell is bound to enter the neighboring cell. This implies, in particular, that the relative roles of auxin efflux and influx carriers (e.g., PIN vs. AUX/LAX proteins) are difficult to distinguish. Recognizing these limitations, Kramer (2004) pioneered the incorporation of intercellular space into auxin transport models. He estimated the range of diffusion

in the intercellular space to be of the same order as the cell size, which could be interpreted as an argument for both including extracellular auxin in more detailed models and excluding it from less detailed models. More recently, intercellular space was postulated to play a fundamental role in the molecular-level models of auxin-based cell polarization proposed by Wabnik et al. (2010), Roussel and Slingerland (2012) and Abley et al. (2013). In addition to auxin itself, candidate molecules involved in auxin-driven patterning involve ABP1 (Napier et al. 2002) and ROP (Xu et al. 2010).

Increasing the spatial resolution of cell models, Kramer (2004) incorporated vacuoles as a factor affecting the diffusion of auxin in the cells, and Hamant et al. (2008) subdivided the cell wall in order to analyze cell wall mechanics with the finite element method. In addition, Hamant et al. (2008) showed a correlation between the orientation of cortical microtubules, which are thought to be sensitive to stresses, and PIN polarity. The likely significant role of mechanosensing creates the need of representing the cytoskeleton in detailed models of auxin patterning as well.

The above representations of cells and tissues are of the Lagrangian type: they describe *where* in space the cells and their components are located. In contrast, Eulerian representations characterize *what* is located in different points in space. An example of the Eulerian viewpoint is the Cellular Potts model (Merks and Glazier 2005), which was employed to simulate auxin distribution and flow in the root of Arabidopsis by Grieneisen et al. (2007). Changes of shape due to deformations or growth are more easily represented from the Lagrangian viewpoint (Fan et al. 2013), which suggests why it has been used more frequently in tissue modeling.

2.3   Static vs. Dynamic Tissue Models

Some models of auxin-based patterning operate on tissues with a fixed geometry: cell arrangements generated programmatically (e.g., Mitchison 1981; Rolland-Lagan and Prusinkiewicz 2005; Feugier et al. 2005) or templates obtained by digitizing a microphotograph (e.g., Barbier de Reuille et al. 2006; Stoma et al. 2008; Bayer et al. 2009; Santuari et al. 2011). The underlying assumption is that the modeled patterning processes are fast compared to tissue growth, and thus growth can be neglected (c.f. Bayer et al. 2009). However, patterning may also be driven by growth or coupled with growth in a feedback loop of interactions. Sample models exploring such connections include phyllotactic patterning in a growing shoot apical meristem (Jönsson et al. 2006; Smith et al. 2006a; O'Connor et al. 2014), the sequential production of serrations in a growing leaf (Bilsborough et al. 2011), and the maintenance of the pattern of auxin flow ("reflux") in a growing Arabidopsis root (Grieneisen et al. 2007; Mironova et al. 2012). Tissue growth can be modeled geometrically, as a consequence of the expansion of the surface in which the cells are embedded (e.g., Smith et al. 2006a), or using a physically based

model (e.g., Jönsson et al. 2006; Merks et al. 2011). In the latter case, cell expansion is attributed to an imbalance between the internal pressure in the cell and cell wall tension (Lockhart 1965; Prusinkiewicz and Lindenmayer 1990). Compared to the geometric models with prescribed growth, physically based models facilitate the inclusion of the impact of patterning on growth. In addition, they inherently incorporate physical forces, which may be morphogenetically relevant due to mechanosensing (Hamant et al. 2008; Heisler et al. 2010).

Models of tissue growth involve cell divisions, which are frequently simulated using the Errera (1886) rule. In the context of auxin-driven patterning, cell divisions pose a problem, because the impact of divisions on auxin transport and the distribution of the transporters is not sufficiently understood. The assumptions that the daughter cells preserve the polarization of the parent cell (Bilsborough et al. 2011) or that the polarization of the daughter cells is immediately established by the neighboring cells (Smith et al. 2006a) have been used in practice.

2.4   The State of the Cell

In most models of auxin-based patterning, each cell is characterized by the concentrations of the relevant substances, e.g., auxin, PIN, AUX/LAX, and CUC. Additional parameters are used to nuance this representation, for example, by indicating the polar allocation of PIN proteins to different sections of the membrane (Sect. 3.4) or by specifying the gradient of auxin concentration within the cell (Mitchison 1981). This level of abstraction is closely related to microscopic observations and is often used in models and their visualizations. Further details can be given by subdividing the cell into compartments and specifying relevant parameters individually for each compartment (Kramer 2004).

It is also possible to account for individual molecules of auxin and other substances (Garnett et al. 2008; Renton et al. 2012), instead of characterizing them summarily as concentrations. Potential advantages of this approach include a more intuitive model of interaction and transport of molecules, and the sustained validity of the model when the numbers of molecules are small and the continuous notion of concentration no longer applies (Gillespie 1976, 1977). At present, the numbers of molecules involved in auxin-driven patterning are not known, and thus it is not clear whether the increased computational cost of simulating individual molecules, compared to solving systems of differential equations used in the continuous case, is justified.

3 Auxin Transport

Auxin-induced patterning in plants is intimately related to auxin distribution and transport, in which auxin efflux carriers from the PIN family (Zažímalová et al. 2010) and auxin influx carriers from the AUX/LAX family (Swarup and Péret 2012) have received the closest attention. The currently recognized key processes involved in auxin transport are shown in Fig. 15.4a. The concentration of PIN on each membrane is determined by allocation (exocytosis, 1) and deallocation (endocytosis, 2) from a pool of free PIN in the cell. PINs located at the membrane export auxin from the cell to the extracellular space (3). From there, auxin is transported back into cells with the help of AUX/LAX proteins (4), which are assumed to be uniformly distributed along the cell membranes. Auxin also moves between the cells and the extracellular space by diffusion and background transport due to the residual presence of auxin exporters along the cell membranes (5). Finally, auxin diffuses between neighboring extracellular compartments (6). If the extracellular space is neglected, there is no extracellular diffusion, and any auxin leaving a cell directly enters the adjacent cell, as shown in Fig. 15.4b.

Below we present the typical equations used to model these processes. We first discuss the case when extracellular space is included and then introduce the simplified equations employed when this space is omitted. For simplicity, we assume that each cell has unit volume and each cell wall has unit area. Extensions to nonuniform volumes and lengths are described, for example, by Smith et al. (2006a), Jönsson et al. (2006), Stoma et al. (2008) and Bayer et al. (2009).

3.1 Auxin Mass Conservation

In cell i, auxin concentration [IAA_i] changes according to the equation:

$$\frac{d[\text{IAA}_i]}{dt} = \text{Production} - \text{Removal} - \text{Flux}. \tag{15.1}$$

The *Production* term accounts for auxin biosynthesis, the level of which has a qualitative impact on some patterning processes (Pinon et al. 2013). The *Removal* term captures auxin turnover or conversion of auxin to a conjugated form. Both these terms may depend on the auxin concentration [IAA_i]. For example, auxin production may have the form of a polynomial or rational polynomial function (e.g., Smith et al. 2006a, Eq. 5), which are easily derived from the chemically plausible laws of mass action (Shapiro et al. 2013). The *Production* term may also incorporate the effect of exogenous application of auxin in simulated experiments (e.g., Smith et al. 2006a), and both the *Production* and *Removal* terms may include sources or sinks representing tissues not explicitly included in the simulation (e.g., Mitchison 1980).
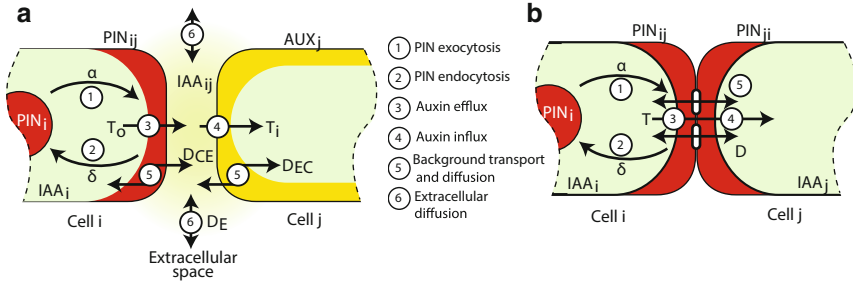
Fig. 15.4 Processes underlying cellular-level models of polar auxin transport with (**a**) and without (**b**) intercellular space. Variables and parameters denoted by letters are explained in Sect. 3

The last term, *Flux*, represents the net flow (difference between outflux and influx) of auxin from cell i. It is the sum of fluxes Φ_{ij} through the membranes of cell i facing cells j in the neighborhood $N(i)$ of cell i:

$$\text{Flux} = \sum_{j \in N(i)} \Phi_{ij}. \qquad (15.2)$$

Cells do not exchange fluxes directly, but via the extracellular space. Auxin concentration $[\text{IAA}_{ij}]$ in the extracellular compartment between cells i and j changes according to the fluxes from cells i and j and diffusion to neighboring extracellular regions:

$$\frac{d[\text{IAA}_{ij}]}{dt} = \Phi_{ij} + \Phi_{ji} - D_{\text{E}} \sum_{(k,l) \in N(i,j)} \left([\text{IAA}_{ij}] - [\text{IAA}_{kl}] \right), \qquad (15.3)$$

where the sum is taken over all extracellular neighbors (k, l) of the extracellular compartment (i, j). The coefficient D_{E} represents the rate of diffusion between adjacent compartments. Fluxes Φ_{ij} through the walls are captured by the chemiosmotic model of auxin transport, described next.

3.2   The Chemiosmotic Model

Inside a cell and within the intercellular space, auxin is assumed to move by diffusion. However, the transport of auxin into and out of cells is more complicated. The chemiosmotic model (Rubery and Sheldrake 1974; Raven 1975; Goldsmith 1977; Mitchison 1980) was proposed to provide a physicochemical basis for the description of this transport.

Auxin is a weak acid, and in the neutral pH inside cells it is largely dissociated. In this ionic form, auxin is hydrophilic and unable to diffuse across the plasma

membrane. In order to leave a cell, auxin requires the activity of carriers located at the plasma membrane (Zažímalová et al. 2010), among which PIN proteins appear to play the most prominent morphogenetic role. Outside the cell, a significant portion of auxin becomes protonated in the lower pH of the extracellular space. This auxin is lipophilic, which makes it able to cross the plasma membrane and diffuse back into cells. Additionally, auxin is transported into cells by the AUX/LAX family of auxin import carriers, located in the plasma membrane.

Equations often used to implement the chemiosmotic model of auxin transport have been presented by Kramer (2009) (see also Kramer 2004; Swarup et al. 2005; Jönsson et al. 2006; Heisler and Jönsson 2006; Sahlin et al. 2009). The flux of auxin from the extracellular space ij into cell i is described as a combination of fluxes due to diffusion—Φ_{diff}, export—Φ_{export}, and import—Φ_{import}:

$$\Phi_{ij} = \Phi_{\mathrm{diff}} + \Phi_{\mathrm{export}} + \Phi_{\mathrm{import}}. \tag{15.4}$$

The flux due to diffusion, Φ_{diff}, is proportional to the difference in concentration of protonated auxin between the cell i and the extracellular space ij. Given pK, the negative log of dissociation constant for auxin, and $\mathrm{pH_c}$, the pH of a compartment c, the protonated proportion of auxin in this compartment is (Weiss 1996):

$$K_{\mathrm{c}}^{\mathrm{IAAH}} = \frac{1}{1 + 10^{\mathrm{pH_c} - \mathrm{pK}}}. \tag{15.5}$$

Flux due to diffusion can thus be calculated as

$$\Phi_{\mathrm{diff}} = P_{\mathrm{diff}} \left(K_i^{\mathrm{IAAH}} [\mathrm{IAA}_i] - K_{ij}^{\mathrm{IAAH}} [\mathrm{IAA}_{ij}] \right), \tag{15.6}$$

where P_{diff} is the membrane permeability for auxin diffusion.

The fluxes due to active transport, Φ_{export} and Φ_{import}, are typically modeled using the Goldman–Hodgkin–Katz equation (Weiss 1996), assuming that the membrane is a homogeneous material and that the permeability to auxin depends on membrane potential. If we let

$$f(z) = \frac{\phi z}{e^{\phi z} - 1} \quad \text{with} \quad \phi = \frac{VF}{RT}, \tag{15.7}$$

where V is the membrane potential, F is the Faraday constant, R is the gas constant, T is the absolute temperature, and z is the net valence of the ions being transported, the equations for import and export can be written as

$$\Phi_{\mathrm{export}} = P_{\mathrm{export}} \left(f(z) K_i^{\mathrm{IAA^-}} [\mathrm{IAA}_i] - f(-z) K_{ij}^{\mathrm{IAA^-}} [\mathrm{IAA}_{ij}] \right), \tag{15.8}$$

$$\Phi_{\text{import}} = P_{\text{import}}\left(f(-z)K_i^{\text{IAA}-}[\text{IAA}_i] - f(z)K_{ij}^{\text{IAA}-}[\text{IAA}_{ij}]\right). \qquad (15.9)$$

In the above equations, we use the notation

$$K_c^{\text{IAA}-} = 1 - K_c^{\text{IAAH}} = \frac{1}{1 + 10^{\text{pK}-\text{pH}_c}}. \qquad (15.10)$$

P_{import} is the membrane permeability for import of auxin by AUX/LAX, and P_{export} is the membrane permeability for the export of auxin by PIN and other exporters, such as the ABCB proteins (Zažímalová et al. 2010). These equations represent diffusion down the electrochemical gradient. Equations (15.8) and (15.9) are similar to Eq. (15.6) except for the factor $f()$ required to account for the dependence of fluxes on membrane potential. P_{import} depends on the membrane concentration of importers $[\text{AUX}_i]$, whereas P_{export} depends on the membrane concentration $[\text{PIN}_{ij}]$ of PIN proteins, as well as on ABCB proteins, which are assumed to be present at a background level (Grieneisen et al. 2007; Kramer 2009).

With a few exceptions (Steinacher et al. 2012; Hošek et al. 2012), the terms in Eqs. (15.5), (15.7), and (15.10) have been assumed constant in simulation models. Kramer (2009) calculated the three fluxes given by Eqs. (15.6), (15.8), and (15.9) by setting $z = 1$, using a membrane voltage of 120 mV, pK = 4.8, pH$_{ij}$ = 5.3, and pH$_i$ = 7.2. This yielded:

$$\begin{aligned}
\Phi_{\text{diff}} &= \left(0.004[\text{IAA}_i] - 0.24[\text{IAA}_{ij}]\right)P_{\text{diff}}, \\
\Phi_{\text{export}} &= \left(4.68[\text{IAA}_i] - 0.034[\text{IAA}_{ij}]\right)P_{\text{export}}, \\
\Phi_{\text{import}} &= \left(0.045[\text{IAA}_i] - 3.57[\text{IAA}_{ij}]\right)P_{\text{import}}.
\end{aligned} \qquad (15.11)$$

A comparison of coefficients in the expression for Φ_{diff} shows that diffusion into the cell is favored over diffusion out of the cell by almost two orders of magnitude. However, the coefficient 3.57 is much larger than the other influx terms (preceded by the minus sign in the equations), which suggests that carrier-mediated influx dominates in cells where importers are expressed (provided that permeabilities P_{diff}, P_{export}, and P_{import} have comparable values). Likewise, of the three terms controlling auxin efflux, coefficient 4.68 of the export term is significantly larger than the other two terms, which is consistent with the biological importance of PIN proteins. Note that the model implies a small influx involving exporters of auxin, and efflux involving its importers.

3.3 Auxin Fluxes

To obtain the typical equations used to model flux through a membrane, Φ_{ij}, we eliminate negligible terms in Eqs. (15.6), (15.8), and (15.9) according to the analysis of Eq. (15.11). Assuming that P_{export} is proportional to $[\text{PIN}_{ij}] + \beta$, where

β is the background concentration of efflux carriers, and P_{import} is proportional to $[\text{AUX}_i]$, we then obtain:

$$
\begin{aligned}
\Phi_{\text{diff}} &= -0.24 P_{\text{diff}} \big[\text{IAA}_{ij}\big], \\
\Phi_{\text{export}} &= 4.68 P_{\text{export}} \big[\text{IAA}_i\big] &= 4.68 K_{\text{PIN}} \big(\big[\text{PIN}_{ij}\big] + \beta\big) \big[\text{IAA}_i\big], \quad (15.12)\\
\Phi_{\text{import}} &= -3.57 P_{\text{import}} \big[\text{IAA}_{ij}\big] &= -3.57 K_{\text{AUX}} [\text{AUX}_i]\big[\text{IAA}_{ij}\big],
\end{aligned}
$$

where K_{PIN} and K_{AUX} are coefficients of proportionality. By combining constant terms and parameters P_{diff}, β, K_{PIN}, and K_{AUX}, we can rewrite the fluxes as

$$
\begin{aligned}
\Phi_{\text{diff}} &= -D_{\text{EC}}\big[\text{IAA}_{ij}\big], \\
\Phi_{\text{export}} &= \big(T_{\text{O}}\big[\text{PIN}_{ij}\big] + D_{\text{CE}}\big)\big[\text{IAA}_i\big], \quad (15.13)\\
\Phi_{\text{import}} &= -T_{\text{I}}[\text{AUX}_i]\big[\text{IAA}_{ij}\big],
\end{aligned}
$$

which, when summed, yield the net flux through the membrane equal to

$$
\Phi_{ij} = T_{\text{O}}\big[\text{PIN}_{ij}\big][\text{IAA}_i] + D_{\text{CE}}[\text{IAA}_i] - D_{\text{EC}}\big[\text{IAA}_{ij}\big] - T_{\text{I}}[\text{AUX}_i]\big[\text{IAA}_{ij}\big]. \quad (15.14)
$$

All the elements of this equation are illustrated in Fig. 15.4. The first term accounts for the transport of auxin from cell i to the extracellular space between cells i and j by PIN, with efficiency T_{O}. It is sometimes assumed that this transport is nonlinear and the efficiency of PIN decreases as the concentration of auxin in cell i increases (Jönsson et al. 2006) or as the concentration of auxin in the adjacent compartment increases (Smith et al. 2006a; Bayer et al. 2009; Roussel and Slingerland 2012; Chitwood et al. 2012). The second and third terms account for background auxin transport into the extracellular space with rate D_{CE} and diffusion from the extracellular space into the cell with rate D_{EC}, respectively. The last term captures active import of auxin from the extracellular space by AUX/LAX proteins, with rate T_{I}. For AUX/LAX the same concentration $[\text{AUX}_i]$ is used for all segments of the cell membrane, as these proteins are typically uniformly localized throughout the membrane.

When extracellular compartments are included, all communication between cells is mediated by the extracellular space. Explicit representation of extracellular space is particularly useful in models including the action of AUX/LAX proteins (Kramer 2004; Wabnik et al. 2010) and those interrogating the fundamental mechanisms that underlie PIN polarization (Kramer 2009; Wabnik et al. 2010; Roussel and Slingerland 2012; Abley et al. 2013). However, in patterning models the extracellular space is often assumed to play a secondary role and is omitted (Fig. 15.4b). In this case, auxin is transported directly between neighboring cells, i.e., every efflux implies a corresponding influx. Equation (15.14) then takes the form:

$$\Phi_{ij} = T\big[\text{PIN}_{ij}\big]\big[\text{IAA}_i\big] - \big[\text{PIN}_{ji}\big]\big[\text{IAA}_j\big] + D\big[\text{IAA}_i\big] - \big[\text{IAA}_j\big]. \qquad (15.15)$$

Equation (15.15) has been used in numerous models, e.g., Mitchison (1981); Smith et al. (2006a); Jönsson et al. (2006); Rolland-Lagan and Prusinkiewicz (2005); Stoma et al. (2008); Feugier et al. (2005); Prusinkiewicz et al. (2009); Bilsborough et al. (2011); O'Connor et al. (2014). The first term accounts for polar transport of auxin from cell i to cell j by PIN located in the membrane of cells i facing j, with efficiency given by T. The second term accounts for polar transport from cell j to cell i in an analogous way. The last two terms account for nonpolar transport between the cells, with rate given by D. They represent the combined effect of phenomena such as diffusion through the extracellular space, background transport of auxin by PIN and other efflux carriers (e.g., ABCB proteins), and diffusion through the plasmodesmata (Rutschow et al. 2011). Note that $\Phi_{ij} = -\Phi_{ji}$, which is not the case when extracellular space is present. Equation (15.15) can be contrasted with that appearing in facilitated diffusion models (Mitchison 1981; Rolland-Lagan and Prusinkiewicz 2005; van Berkel et al. 2013), which postulate regulated permeability of the cell membranes instead of polar auxin transport controlled by the membrane concentration of influx and efflux carriers. In terms of Eq. (15.15), T is then equal to 0, and the values of D change locally as a function of the absolute value of Φ_{ij}. Unlike polar transport, facilitated diffusion cannot move auxin up a concentration gradient.

3.4 PIN Cycling

The concentration of PIN in the membrane of cell i abutting cell j changes due to allocation from (exocytosis) and deallocation to (endocytosis) a pool of unallocated PIN in the cell i:

$$\frac{d\big[\text{PIN}_{ij}\big]}{dt} = \alpha[\text{PIN}_i] - \delta\big[\text{PIN}_{ij}\big]. \qquad (15.16)$$

Here $[\text{PIN}_i]$ denotes PIN concentration within the cell, α is the rate of exocytosis, and δ is the rate of endocytosis. These rates may depend on several factors. For α, typical examples include auxin concentration in the neighboring cell j (Smith et al. 2006a; Jönsson et al. 2006; Bayer et al. 2009; Bilsborough et al. 2011; Draelants et al. 2012; O'Connor et al. 2014) and auxin flux through the membrane (Feugier et al. 2005; Stoma et al. 2008; Bayer et al. 2009; Farcot and Yuan 2013; O'Connor et al. 2014). In contrast, δ may be a function of cellular auxin concentration (Paciorek et al. 2005) and also likely depends on cytokinin (Marhavý et al. 2011). Bilsborough et al. (2011) postulated that CUC2 may be required in some instances to modify cellular PIN polarizations, which could be accomplished by acting on α and δ. A broad survey of the various PIN allocation schemes

proposed in the literature is provided by van Berkel et al. (2013), who examined properties of these schemes at the level of cell membranes, cells, and one-dimensional files of cells.

Balancing the allocation of PIN proteins to the cell membranes, the change in concentration of PIN in the cytosol is

$$\frac{d[\text{PIN}_i]}{dt} = -\sum_{j \in N(i)} \frac{d[\text{PIN}_{ij}]}{dt}. \tag{15.17}$$

Initial models of polar auxin transport did not employ Eqs. (15.16) and (15.17), and instead assumed independent production of PIN-like efflux carriers at different segments of the cell membrane (Mitchison 1981; Rolland-Lagan and Prusinkiewicz 2005). However, competitive allocation of PIN proteins from a common pool appears to be more justified in view of biological data (Geldner et al. 2001), and readily leads to high auxin concentrations in developing veins (Feugier et al. 2005), consistent with observations (Sect. 4.2). Recent mathematical analysis (van Berkel et al. 2013; Farcot and Yuan 2013) shows that competitive allocation increases the range of parameters for which stable pattern formation may occur.

4   Elements of Auxin-Based Patterning

Molecular-level observations suggest that auxin regulates its own transport through a feedback with PIN proteins (Reinhardt et al. 2003; Scarpella et al. 2006; Hay et al. 2006; Bayer et al. 2009) (Fig. 15.5). This feedback likely provides the basis for the self-organized patterning of many elements of plant anatomy (Reinhardt et al. 2003; Scarpella et al. 2006; Hay et al. 2006; Barkoulas et al. 2008; Bayer et al. 2009; Bilsborough et al. 2011; O'Connor et al. 2014). Two different types of feedback between auxin and the cellular localization of PIN have been proposed, not precluding a possibility that they are different manifestations of a common mechanism. On the one hand, leaf primordia, as well as serrations, lobes, and leaflets, are initiated at auxin maxima (as inferred through auxin reporters such as DR5), with PIN1 in surrounding tissues polarized towards these maxima (Reinhardt et al. 2003; Hay et al. 2006; Koenig et al. 2009; Barkoulas et al. 2008; Bayer et al. 2009; Bilsborough et al. 2011; O'Connor et al. 2014). This has led to the hypothesis that PIN polarizes *up the gradient* of auxin concentration to generate convergence points (Jönsson et al. 2006; Smith et al. 2006a). On the other hand, during vascular initiation, PIN1 expression is refined into highly polarized strands (Scarpella et al. 2006; Bayer et al. 2009; O'Connor et al. 2014). The patterning of these strands is generally consistent with the canalization hypothesis proposed by Sachs (1969, 1981), according to which auxin flux through cells increases their capacity to transport auxin. The corresponding computational models thus assume that PIN polarizes *with the flux* of auxin transport (Mitchison 1980, 1981;
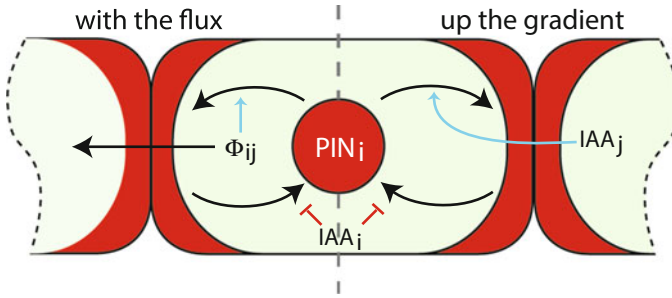
Fig. 15.5 Hypothetical feedbacks controlling the localization of PIN proteins. With-the-flux models assume that (positive) auxin flux Φ_{ij} (c.f. Eq. 15.15) through a cell membrane increases exocytosis, whereas up-the-gradient models assume that high auxin concentration [IAA$_j$] in the adjoining cell increases exocytosis. Some models also assume that cellular auxin concentration [IAA$_i$] inhibits endocytosis

Rolland-Lagan and Prusinkiewicz 2005; Feugier et al. 2005; Fujita and Mochizuki 2006; Stoma et al. 2008; Bayer et al. 2009; O'Connor et al. 2014). Computational models employing these two types of feedback reproduce a broad range of the observed spatiotemporal patterns of auxin signaling and PIN polarization.

4.1 Up-the-Gradient Models

In up-the-gradient models, PIN is allocated to each cell membrane according to the auxin concentration in the neighboring cell (Fig. 15.5). This causes small differences in cellular auxin concentration to be amplified, leading to the emergence of a stable pattern of periodic auxin maxima (Jönsson et al. 2006; Smith et al. 2006a; Sahlin et al. 2009; Draelants et al. 2012; van Berkel et al. 2013). Formally, up-the-gradient polarization can be enacted by making the rate of exocytosis, α in Eq. (15.16), an increasing function of auxin concentration in the neighboring cell j, while keeping the rate of endocytosis δ constant. As noted by Sahlin et al. (2009, p. 66), the opposite case, where the rate of exocytosis is constant and the rate of endocytosis is regulated, is mathematically equivalent; what matters is the ratio between both processes.

In up-the-gradient models constructed to date, PIN polarization has been assumed to be fast compared to the production and turnover of PINs, as well as changes in cellular auxin concentration. Consequently, the concentrations of PIN at each cell membrane and inside each cell were set to their steady-state values at each simulation step:

$$[\text{PIN}_{ij}] = \frac{\alpha\big([\text{IAA}_j]\big)}{\sum_{k \in N(i)} \alpha([\text{IAA}_k]) + \delta}, \qquad (15.18)$$

$$[\text{PIN}_i] = \frac{\delta}{\sum_{k \in N(i)} \alpha([\text{IAA}_k]) + \delta}. \qquad (15.19)$$

These equations can be derived by assuming that the total amount of PIN proteins in the cell, $[\text{PIN}_i] + \sum_{j \in N(i)} [\text{PIN}_{ij}]$, is constant, and setting Eqs. (15.16) and (15.17) to 0 (see Jönsson et al. (2006) for details). A key difference in initial models was the choice of the function $\alpha([\text{IAA}_j])$ relating the rate of PIN allocation to a membrane to the auxin concentration in the abutting cell. Jönsson et al. (2006) employed a Hill function and Smith et al. (2006a) an exponential function. Simulations and mathematical analysis showed that, with either function, up-the-gradient polarization can generate one- and two-dimensional periodic patterns of approximately equidistant auxin maxima (Jönsson et al. 2006; Smith et al. 2006a; Sahlin et al. 2009; Draelants et al. 2012; van Berkel et al. 2013) (Fig. 15.6a, b). Different spacings can be achieved by adjusting model parameters, with the number of cells between peaks depending on the efficiency of polar auxin transport T compared to diffusion rate D (Eq. 15.15) (Fig. 15.6c). Further analysis in two dimensions showed that up-the-gradient models are also capable of creating striped patterns (Sahlin et al. 2009), similar to those emerging in reaction–diffusion models (Meinhardt 1982; Chap. 12). Differentiating between variants of up-the-gradient polarization models, recent mathematical analysis by Draelants et al. (2012) demonstrated that the model of Smith et al. (2006a) can produce oscillating steady states and confirmed the observation by Jönsson et al. (2006) that their model cannot.

Vieten et al. (2005) reported strong upregulation of *PIN1* expression at the sites of primordia initiation, suggesting the dependence of PIN1 production on auxin. Model studies by Smith et al. (2006a) and Heisler and Jönsson (2006) showed that such an upregulation can destabilize auxin peaks. Specifically, if PIN levels increase with auxin concentration, a cell with a high concentration of auxin will also have a high concentration of PIN, resulting in a large outflux of auxin. This may cause the maximum to shift to neighboring cells, which Smith et al. (2006a) and Heisler and Jönsson (2006) found undesirable in the context of phyllotactic patterning. In contrast, Merks et al. (2007) exploited the instability of auxin peaks, motivated by the appeal of a unified model potentially explaining both the formation of convergence points and vascular strands. In their model, the auxin maximum that initiates a leaf primordium subsequently moves into subepidermal tissues. PIN polarity follows this moving peak, leaving behind a strand of polarized PINs patterning a future vein. Unfortunately, predictions of this model are not consistent with the observed spatiotemporal patterns of auxin maxima and PIN polarization in developing leaves. For example, the predicted progression of the auxin maximum from the leaf tip towards the base during midvein formation is not observed in Arabidopsis leaves, where the maximum indicated by the DR5 reporter remains at
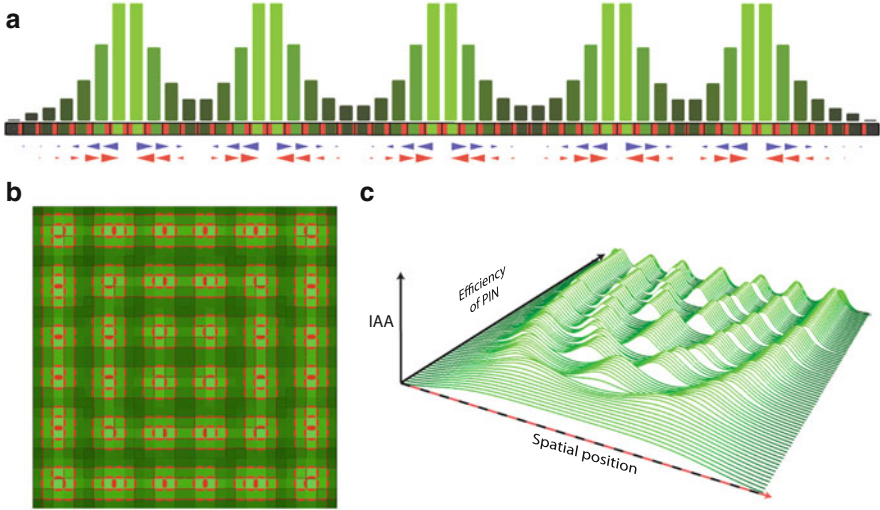
Fig. 15.6 Up-the-gradient patterning. (**a**) One-dimensional pattern of equidistant auxin peaks that emerge when PINs orient up the gradient of auxin concentration. PIN polarization in each cell is shown in *red* and auxin concentration in *green*. Polar transport up the auxin gradient (*red arrows*) balances diffusion down the gradient (*blue arrows*) in the steady state shown. (**b**) A two-dimensional counterpart of the simulation from (**a**) also produces a pattern of auxin peaks. (**c**) The steady-state auxin concentration in a row of 50 cells plotted as a function of the efficiency of PIN transport T (Eq. 15.15). *Red* and *black dashes* indicate the approximate size and position of each cell. As the efficiency of transport increases, the number of maxima increases as well

the tip as the midvein develops. Consequently, most models of vein patterning assume a different mode of PIN polarization, discussed next.

4.2 With-the-Flux Models

In with-the-flux models, PIN allocation to a cell membrane is promoted by auxin flux through this membrane. With-the-flux polarization is the cornerstone of the canalization hypothesis formulated by Sachs (1969, 1981, 1991, 2003). Historically, it was the first conceptual model of patterning that involved auxin and postulated the feedback of auxin on its own transport.

Sachs postulated that the export of auxin across a cell membrane promotes further auxin transport in the same direction and hypothesized that this feedback creates canals of auxin flow in a manner analogous to the carving of riverbeds by flowing water (Sachs 2003). Using a computational model operating on a square array of cells, Mitchison (1980, 1981) showed that the with-the-flux polarization model proposed by Sachs can indeed generate canals of high auxin flux. A reimplementation of Mitchison's model by Rolland-Lagan and Prusinkiewicz (2005) (Fig. 15.7a) and its reinterpretation in terms of a feedback between auxin
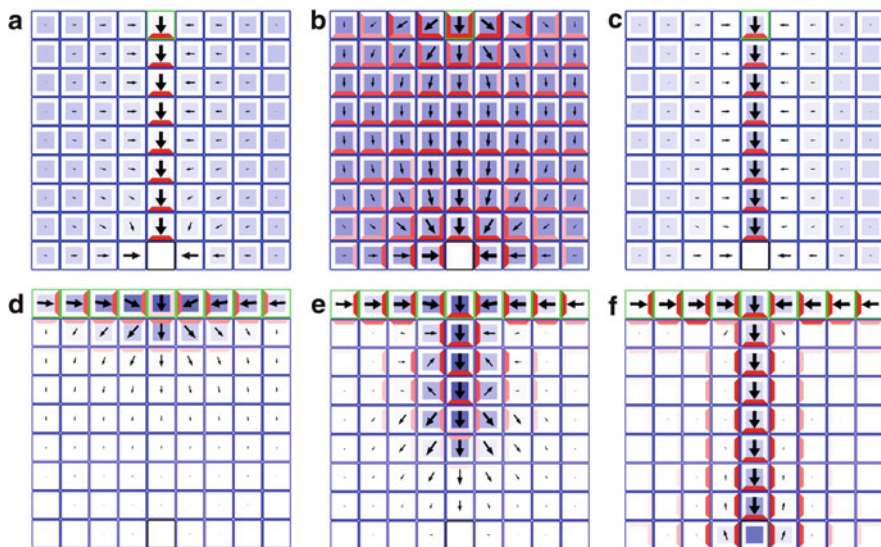
Fig. 15.7 Patterns generated by with-the-flux (**a–c**) and dual-polarization (**d–f**) models. (**a**) A reimplementation (Rolland-Lagan and Prusinkiewicz 2005) of the model proposed by Mitchison (1980). PINs (*red*) are allocated assuming a quadratic dependence on auxin flux (*black arrows*). A canal of polarized cells is formed, connecting the auxin source at the top of the grid (outlined in *green*) to the sink at the bottom (middle cell, bottom row). The canal is characterized by high flux and low concentration of auxin (*blue*). (**b**) A linear PIN allocation function results in a broad coordination of PIN polarity across the tissue. (**c**) An implementation of the canalization model of Feugier et al. (2005). In contrast to panel (**a**), PINs are drawn from a limited pool, causing transport to saturate and auxin to build up in the strand. (**d–f**) Three frames of a simulation using the dual-polarization model by Bayer et al. (2009). (**d**) Epidermal cells (top row) initially polarize up the gradient, causing a convergence point to form in the center of the top row. (**e**) As auxin levels increase, the peak extends into the inner tissue. (**f**) The resulting strand elongates until it reaches the sink

flow and polarization of PIN1 proteins confirmed that the canalization hypothesis is generally consistent with observations of vein formation in developing leaves.

Mitchison (1980) proposed two main variants of his model: facilitated diffusion and polar transport. Each variant suggested a different molecular mechanism. In the case of facilitated diffusion, transport was affected by passive channels. The diffusion rate between cells was assumed to increase with net auxin flux, irrespective of the flux direction. Mitchison (1980) suggested plasmodesmata as potential candidates for the channels. Although it is likely that auxin can move through plasmodesmata to some extent (Rutschow et al. 2011), experimental support for a feedback based on auxin flux is currently lacking.

Polar transport is more compatible with the chemiosmotic model of auxin transport and molecular data on the localization and polarity of the PIN proteins (Rolland-Lagan and Prusinkiewicz 2005). At the cellular level, the impact of auxin

on carrier allocation is captured by making parameter α in Eq. (15.16) a function of the net flux through the cell membrane:

$$\alpha(\Phi_{ij}) = \begin{cases} h(\Phi_{ij}) & \Phi_{ij} \geq 0 \\ 0 & \text{otherwise} \end{cases}, \tag{15.20}$$

where $h(\Phi_{ij})$ is an increasing function of net flux. According to this equation, the export of auxin across a cell membrane promotes further auxin transport in the same direction. Mitchison (1980) used a quadratic allocation function $h(\Phi_{ij})$ (Fig. 15.7a) and reported that it must be supralinear for canalization to occur. This feature was later investigated by Feugier et al. (2005) who found that a variety of supralinear functions for carrier allocation produced strands, including a step function. Feugier et al. (2005) also showed that if allocation is linear or sublinear then broad patterns of coordinated polarity over many cells arise (Fig. 15.7b). Stoma et al. (2008) exploited this regime in a model which, similar to the model of Merks et al. (2007), attempted to encompass phyllotaxis and vein formation using a common mechanism. In this model, linear polarization was assumed in the epidermis of the shoot apical meristem, producing broad patterns of PIN polarization towards primordia, and quadratic polarization was used to model the subepidermal patterning of veins. The produced patterns of PIN polarization closely matched those observed in the shoot apical meristem, but the model predicted a decrease of auxin concentration at the tips of leaf primordia that did not match auxin patterns reported by DR5.

Mitchison's model produces canals with high flux and low concentration of auxin (Fig. 15.7a), whereas experiments suggest that auxin concentration in canals is high (Scarpella et al. 2006). Exploring this discrepancy, Feugier et al. (2005) proposed and analyzed variants of Mitchison's models that operated according to two scenarios: with PINs allocated to different membrane sectors independently, and with PINs allocated to membranes from a fixed pool within each cell (c.f. Sect. 3.4). In the first case, simulations confirmed that the concentration of auxin in canals was lower than in the surrounding tissue, as originally predicted by Mitchison's model. In contrast, when cell membranes competed for the PINs within each cell, the models produced canals with auxin concentration higher than in the surrounding tissue (Fig. 15.7c). This result removed a key inconsistency between the canalization hypothesis and experimental data.

Competitive allocation of PIN qualitatively modifies the results of simulation compared to the noncompetitive allocation for the following reason. Given the fixed pool of PIN proteins in a cell, competitive allocation of PIN to one segment of the membrane (bottom segment of the provascular cells in Fig. 15.7c) reduces PIN allocation to the remaining segments of the membrane in the same cell. Consequently, auxin outflux from the provascular strand is reduced. From the viewpoint of the cells adjacent to this strand, this situation is indistinguishable from the reduction of outflux due to low concentration of auxin in Mitchison's model (Fig. 15.7a). This can be seen by rewriting Eq. (15.15) into the form:

$$\Phi_{ij} = \left(T\left[\text{PIN}_{ij}\right] + D\right)\left[\text{IAA}_i\right] - \left(T\left[\text{PIN}_{ji}\right] + D\right)\left[\text{IAA}_j\right]. \tag{15.21}$$

Reduction in the concentration of $[\text{PIN}_{ji}]$ postulated by Feugier's model, but not by Mitchison's model, has the same effect on the flux Φ_{ij} as a reduction of auxin concentration $[\text{IAA}_j]$.

4.3 The Dual-Polarization Model

The proposed modes of PIN polarization by auxin, up the gradient and with the flux, involve the same molecular players. This raises the question of how a plant decides where and when to deploy each mode. Addressing this question, Bayer et al. (2009) investigated the development of the midvein in tomato leaf primordia. There the auxin peak that causes leaf initiation in the meristem remains in place while the strand that prepatterns the midvein is formed. To explain these dynamics, Bayer et al. (2009) proposed a dual-polarization model, according to which up-the-gradient and with-the-flux modes operate concurrently, with the weights dependent on the tissue type and auxin concentration. Figure 15.7d–f shows a simulation of this model. At first, auxin levels are low, allowing PINs to polarize up the gradient in the L1 and form a new convergence point (Fig. 15.7d). As the auxin levels increase, cells at the convergence point begin to favor with-the-flux polarization, which directs auxin flow towards inner tissues. This causes the peak to extend into a canal that eventually connects the source to the sink (Fig. 15.7e, f). The model reliably produces canals with high auxin concentration, as any drop in concentration would restore the up-the-gradient polarization mode, replenishing auxin in the canal.

The existence of an auxin-dependent transition between these two modes of PIN1 polarization has recently been supported by Furutani et al. (2014), who showed that genes from the *MAB4* family mediate the transition from up-the-gradient PIN1 polarization at lower auxin concentrations to with-the-flux polarization at higher concentrations. An interesting hypothesis is that PINOID is also involved in the deployment of each mode (van Berkel et al. 2013), as it is known to regulate apical vs. basal polarization of members of the PIN family in the root (Friml et al. 2004) in a manner dependent on auxin (Fozard et al. 2013).

The work of Bayer et al. (2009) suggests that the combined action of the up-the-gradient and with-the-flux polarization modes suffices to explain patterning induced by polar auxin transport in the shoot. Further support for the coordinated operation of up-the-gradient and with-the-flux polarization modes is presented by (O'Connor et al. 2014), who showed that in grasses these modes of polarization may be associated with distinct proteins related to AtPIN1 (c.f. Sect. 5.3).

4.4   The Role of Import Carriers

In addition to export carriers, the flow of auxin is affected by the AUX/LAX family of import carriers (Bennett et al. 1996; Parry et al. 2001) (Eqs. 15.11, 15.12, 15.13 and 15.14). These proteins are typically, although not always (Swarup et al. 2001), located uniformly on the cell membranes. Experimental results and models have focused on the role of AUX/LAX in enhancing and maintaining patterns of high auxin concentration in selected cells, vascular strands, and tissues. In contrast, studies of PINs have been focused on their primary role in the self-organization of patterns.

The first computational model by Kramer (2004) showed that AUX/LAX proteins can contribute to the maintenance of high auxin concentrations in vascular strands. A subsequent model by Swarup et al. (2005) pointed to the importance of AUX/LAX proteins in maintaining gradients of auxin concentration that are responsible for gravitropic responses in the root. Heisler and Jönsson (2006) used computational models to support the hypothesis that AUX/LAX proteins play a role concentrating auxin in the epidermis of shoot apical meristems (Reinhardt et al. 2003), although the retention or concentration of auxin in the epidermis also involves PIN1 (Bainbridge et al. 2008; Bayer et al. 2009; Kierzkowski et al. 2013). Heisler and Jönsson (2006) and Sahlin et al. (2009) also showed that auxin-induced AUX/LAX proteins may help to fix auxin maxima at the locations at which they emerged (i.e., the convergence points), and thus stabilize phyllotactic patterns. This role of AUX/LAX is consistent with the observations of irregular phyllotaxis patterns in plants with multiple mutations of these importers (Bainbridge et al. 2008).

Auxin application has been shown to upregulate AUX1 in roots (Laskowski et al. 2006, 2008; Paponov et al. 2008). On this basis, Laskowski et al. (2008) proposed that a positive feedback between auxin and its importers in the pericycle reinforces auxin peaks during lateral root initiation. Smith and Bayer (2009) explored this idea further using a model of a line of cells. They showed that a positive feedback between auxin-dependent importer production and the retention of auxin by importers not only can reinforce preexisting patterns, but can also generate patterns of equidistant peaks de novo (Fig. 15.8). These patterns resemble those generated by up-the-gradient polar transport of auxin by PIN (Fig. 15.6a). In contrast to peak formation by PIN proteins, peak formation by auxin importers does not require polarized transporters.

4.5   Molecular Basis of Cell Polarization

Although formulated in molecular terms, neither the up-the-gradient nor with-the-flux model explains the molecular mechanism of PIN polarization. As experimental data remain limited, several computational models have recently been proposed to
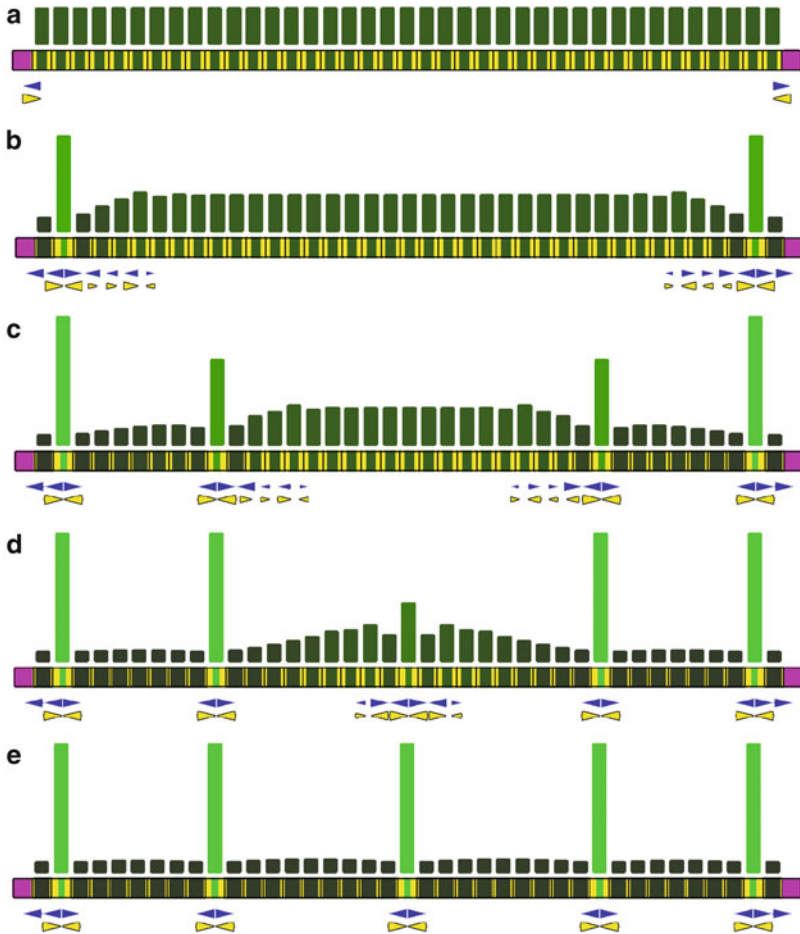
Fig. 15.8 One-dimensional simulation of a hypothetical pattern formation process driven by AUX/LAX. Panels (**a–e**) represent subsequent stages of the simulation. Auxin concentration in each cell is shown in *green* and AUX/LAX concentration on cell membranes in *yellow*. Auxin is produced at the same rate in each cell. The first and last cells, shown in *purple*, are auxin sinks. The concentration of AUX/LAX is a quadratic function of auxin concentration. As cellular auxin levels increase, influx due to AUX/LAX (*yellow arrows*) begins to exceed efflux due to diffusion or transport by background efflux carriers (*blue arrows*), leading to auxin accumulation in some cells (progression from **a** to **b**). A competition between cells results, where the cells achieving a high auxin concentration deplete auxin from nearby cells. A pattern of approximately equidistant auxin maxima gradually emerges (**c, d, e**)

explore hypothetical mechanisms. Generally, these models can be divided into two classes: those postulating a purely biochemical polarization mechanism (Kramer 2009; Wabnik et al. 2010; Roussel and Slingerland 2012; Abley et al. 2013) and those incorporating biomechanical factors (Heisler et al. 2010).
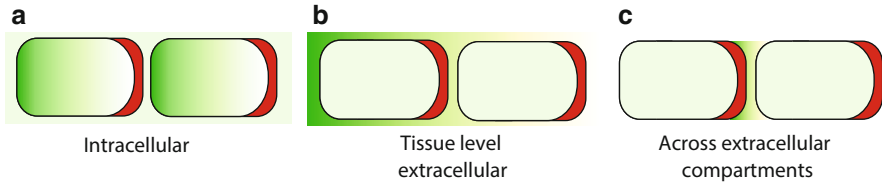
Fig. 15.9 Auxin concentration gradients assumed in postulated molecular-level models of PIN polarization. High auxin concentrations are shown in *green* and low in *white*. (**a**) Gradients are present in individual cells (Kramer 2009). (**b**) Tissue-level gradient are present in the extracellular space (Roussel and Slingerland 2012; Abley et al. 2013). (**c**) Gradients are present in compartments of the extracellular space (Wabnik et al. 2010)

The biochemical models explore the emergence of a coherent polarization in a set of cells under different assumptions regarding auxin gradients. These assumptions include emergent coordination of auxin gradients in individual cells (Fig. 15.9a), alignment of polarizations governed by a tissue-level gradient in the intercellular space (Fig. 15.9b), and transmission of polarizing information via auxin gradients in the extracellular spaces between adjoining cells (Fig. 15.9c).

Kramer (2009) explored Mitchison's (1981) idea that flux sensing could result from a readout of intracellular auxin gradients (Fig. 15.9a). He suggested a role for the auxin-binding protein ABP1 in sensing these gradients, and showed that the resulting auxin fluxes can become canalized. In the reported simulations, vascular strands were always initiated at auxin sinks. In contrast, experimental observations suggest that the midvein in the leaf is initiated at an auxin source (Scarpella et al. 2006; Bayer et al. 2009; O'Connor et al. 2014). Kramer (2009) did not comment whether his model could reproduce these dynamics as well.

Roussel and Slingerland (2012) investigated another model of PIN polarization. They postulated that auxin in the extracellular space inhibits PIN exocytosis and, consequently, PIN proteins polarize towards regions of low auxin concentration in the extracellular space (Fig. 15.9b). This model produced a tissue-scale gradient of extracellular auxin spanning its source and sink, with PINs in the cells polarized consistently towards the sink. The source and the sink were connected by a path of high auxin flux in a manner resembling a vein, but auxin concentration in this path was not consistently elevated, in contrast to experimental data (c.f. Sect. 4.2).

Abley et al. (2013) systematically explored several hypothetical mechanisms that potentially could underlie cell polarization in both animals and plants. The mechanism they proposed to describe polarization in plants employed a PIN-like transporter molecule and an auxin-like substance that was exported from cells into the extracellular space by the transporter molecule. The extracellular auxin promoted PIN endocytosis, thus decreasing PIN concentration on both membranes abutting the same extracellular compartment. An inherent part of the model is the assumption of two antagonistic membrane-bound substances (possibly the proteins ROP2 and ROP6), one of which correlates positively and another one negatively with the localization of PIN. These substances enforce inherent cell polarization

even in the absence of external stimuli. Abley et al. showed that a coordinated polarization of cells in a tissue results, and the steady-state auxin concentration in consecutive cells may either decrease or increase towards the sink, depending on model parameters. They did not apply their model to specific patterning processes, such as the formation of convergence points or veins.

In both the models of Roussel and Slingerland (2012) and Abley et al. (2013), auxin in the extracellular space acted symmetrically on the adjacent cells. In contrast, Wabnik et al. (2010) proposed that auxin in the extracellular compartments forms gradients, and these gradients provide asymmetric cues guiding PIN polarization in the adjacent cells (Fig. 15.9c). Similar to Kramer (2009), Wabnik et al. (2010) postulated that the auxin-binding protein ABP1 plays a role in this process, but they assumed that ABP1 interacts with auxin in the apoplast rather than within cells. PIN polarization would thus emerge from the intercellular competition for the ABP1 proteins that prevent PIN endocytosis. This hypothesis is consistent with experimental data showing that ABP1 is secreted from the cell where it is physiologically active (Napier et al. 2002) and is involved in the inhibition of endocytosis by auxin (Robert et al. 2010). The resulting model reproduced numerous details of vascular patterning and regeneration. Furthermore, bifurcation analysis indicated that it was capable of transitioning between up-the-gradient and with-the-flux transport regimes. Potentially, it could thus also account for phyllotaxis and other up-the-gradient phenomena. Nevertheless, the question remains whether significant auxin gradients are possible in the very narrow spaces between cells in the tissues where patterning occurs.

A model assuming that PINs are polarized by mechanical forces was proposed by Heisler et al. (2010), who built on their earlier model (Hamant et al. 2008) to explain peak formation in the shoot apex. Heisler et al. showed that PIN polarity is correlated with microtubule patterns, which can be modified by mechanical stresses. They proposed that high auxin concentration in a cell causes its wall to loosen, transferring load onto the wall of the adjacent cell (the loads acting on adjacent cell walls, abutting the same extracellular compartment, may thus be different). These stresses were sensed by the cells and used as a cue to polarize PIN proteins. Using a computational model operating on a fixed template of hexagonal cells, Heisler et al. (2010) showed that the feedback between the polarization of PIN proteins and stresses can generate a whorled pattern of auxin maxima.

Mechanical forces have also been involved in models of vascular patterning in leaves (Couder et al. 2002; Laguna et al. 2008; Corson et al. 2009), but links between these models and polar auxin transport are tenuous.

5 Review of Specific Models

A tight synergy between laboratory experiments and computational models underlies recent studies of growth regulation and patterning focused on the role of auxin. The fountain model (Fig. 15.1) suggests an exciting possibility of reducing fundamental features of plant development to a small number of general mechanisms. At a more immediate level, it presents a structured set of hypotheses regarding some of the key elements of plant development. Below we discuss these elements in more detail.

5.1 Phyllotaxis

The first morphogenetic process involving auxin, in the order implied by the reverse fountain model, is the generation of a phyllotactic pattern of leaf and flower primordia on the shoot apical meristem (SAM). Microscopic observations of meristems in Arabidopsis by Reinhardt et al. (2003) showed that PIN1 proteins are oriented towards spatially separated convergence points, creating auxin maxima that predict the location of new primordia. Following these observations, they proposed that phyllotactic patterns emerge from a competition for auxin, where existing primordia drain auxin from their neighborhoods. This creates zones of low auxin concentration surrounding each primordium, where new primordia cannot be formed. The conceptual model of Reinhardt et al. can thus be viewed as a molecular implementation of the inhibitory mechanism of phyllotaxis proposed by Hofmeister (1868): the absence of auxin plays the role of an inhibitor. It leaves open, however, the question of what information is used to polarize PINs towards a convergence point, and what biochemical or biomechanical mechanisms effect this polarization. Addressing the first question, Jönsson et al. (2006) and Smith et al. (2006a) postulated a feedback between auxin distribution and PIN localization. According to these models, active auxin transport by PIN proteins creates auxin maxima that localize the incipient primordia. PINs orient themselves preferentially towards these maxima, promoting further auxin flux that reinforces them (up-the-gradient model, c.f. Sect. 4.1). Operating on a growing surface approximating the shoot apical meristem, this basic mechanism creates a relatively irregular pattern of auxin maxima. However, with additional assumptions—the restriction of the initiation of new primordia to the peripheral zone, the immobilization of auxin maxima, and the strengthening of PIN1 polarization towards the incipient primordia after their initiation (Smith et al. 2006a)—the model generates typical, highly regular spiral phyllotactic patterns (Fig. 15.10). Van Mourik et al. (2012) have recently proposed a related model to explain the patterning of floral organ primordia in Arabidopsis.

Motivated by the auxin-driven models of phyllotaxis, Smith et al. (2006b) and Mirabet et al. (2012) analyzed the robustness of phyllotactic patterning using models that abstract inhibitory properties of auxin in geometric terms. Both studies
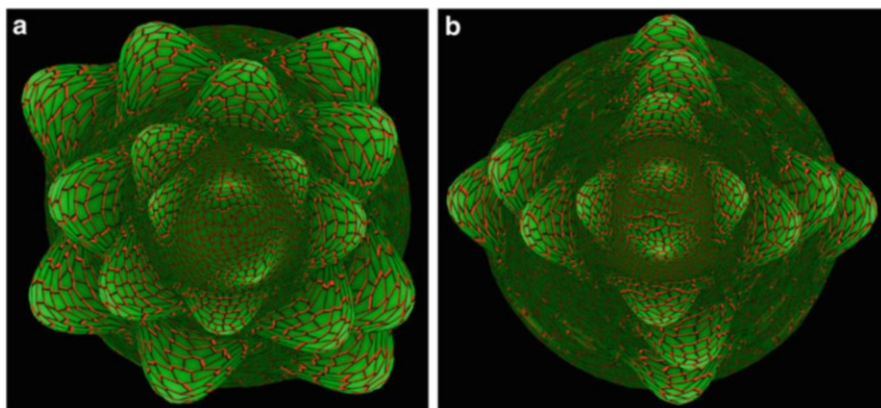
Fig. 15.10 Simulation model of organ formation in the shoot apical meristem (Smith et al. 2006a). Transport of auxin (*green*) by PIN proteins (*red*) creates a self-organizing pattern of auxin maxima. PINs are polarized up the gradient, resulting in a spacing mechanism that positions auxin peaks as far as possible from previously existing ones. These peaks trigger the formation of new organs that bulge out from the apex surface. Growth of the shoot apex creates space at the tip, giving room for new organs to appear. Depending on model parameters and initial conditions, this can lead to a pattern of spiral (**a**) or decussate (**b**) phyllotaxis

postulated a secondary inhibitory field as a means through which the robustness of phyllotactic pattern formation can be increased. The more detailed analysis by Mirabet et al. (2012) has also considered a form of instability manifested by incorrect order of the initiation of primordia. Besnard et al. (2014) have subsequently shown that cytokinin establishes a secondary field which reduces the frequency of such instabilities in Arabidopsis. In addition to the inherent value of these results, they point to the need and usefulness of extending auxin-driven models with other regulatory processes and substances.

5.2   Leaf Development

Once positioned, a leaf primordium begins to grow, bulging out of the shoot apical meristem and gradually flattening along the abaxial–adaxial axis. During this growth, new convergence points emerge along the leaf margin, while the convergence point that initiated the leaf remains at the leaf tip (Scarpella et al. 2006; Hay et al. 2006). The formation of convergence points along the leaf margin appears to be governed by a mechanism similar to phyllotactic patterning in the SAM (Berleth et al. 2007; Smith and Bayer 2009; Bilsborough et al. 2011). As in phyllotaxis, existing convergence points locally inhibit the formation of new convergence points by draining auxin. New points thus only emerge when sufficient space is created for them by leaf growth. Similar to their counterparts at the shoot apical meristem, the convergence points at the leaf margin mark locations of increased

outgrowth, yielding serrations in the case of Arabidopsis leaves (Bilsborough et al. 2011) and, possibly, lobes in leaves of other species (Barkoulas et al. 2008; Koenig et al. 2009). This similarity is consistent with the "partial shoot theory" (Arber 1950), which emphasizes parallels between the growth of shoots and leaves (Champagne and Sinha 2004). Following this train of thought, the strikingly different appearance of spiral phyllotactic patterns and leaves does not result from fundamentally different morphogenetic processes, but from the different geometries on which they operate: an approximately paraboloid shoot apical meristem that dynamically maintains its form vs. a flattening leaf that changes its shape and size as it grows.

Bilsborough et al. (2011) constructed a computational model of Arabidopsis leaf serration to further explore leaf development (Fig. 15.11). The general features of the observed serration patterns could be explained in terms of a feedback between auxin and PIN proteins, but the model showed that an additional factor was required to stabilize auxin maxima and thus robustly position serrations (Fig. 15.11b, c). This stabilizing role was fulfilled by the CUC2 protein, known to play a major role in leaf serration development (Nikovics et al. 2006; Kawamura et al. 2010). Following experimental data (PIN1 convergence points do not form in *cuc2* mutants), Bilsborough et al. (2011) hypothesized that PIN1 repolarization may only occur in the presence of CUC2. Auxin, however, downregulates *CUC2* expression, thus fixing PIN1 localization at the convergence points. It is an interesting question whether a related mechanism also stabilizes auxin maxima during phyllotactic pattern generation at the SAM [as suggested by Nikovics et al. (2006) and Berger et al. (2009)].

Chitwood et al. (2012) observed that auxin maxima in the model of phyllotaxis by Smith et al. (2006a) have an asymmetric shape and hypothesized that this asymmetry may disrupt the bilateral symmetry of leaf forms. They validated this hypothesis experimentally in tomato. Specifically, they observed the predicted asymmetric DR5 expression due to differences in distances between a given maximum and adjacent primordia in the clockwise and counterclockwise directions around the shoot and confirmed a relation between the direction of phyllotaxis (clockwise or counterclockwise) and the resulting asymmetry of leaves using a statistical analysis of leaf form.

5.3   Vascular Patterning

The models of phyllotaxis and leaf formation discussed above operate at the boundary of the organs considered: in the epidermis of the shoot apical meristem and at the margin of the leaf. The localization of PIN1 proteins and the activation of the DR5 auxin reporter in emerging leaves indicate that auxin reaching convergence points is redirected there towards the leaf interior. Its flow is then organized into canals: narrow paths that define the position of future veins. Modeling of vein formation is intimately linked with auxin canalization discussed in Sect. 4.2.
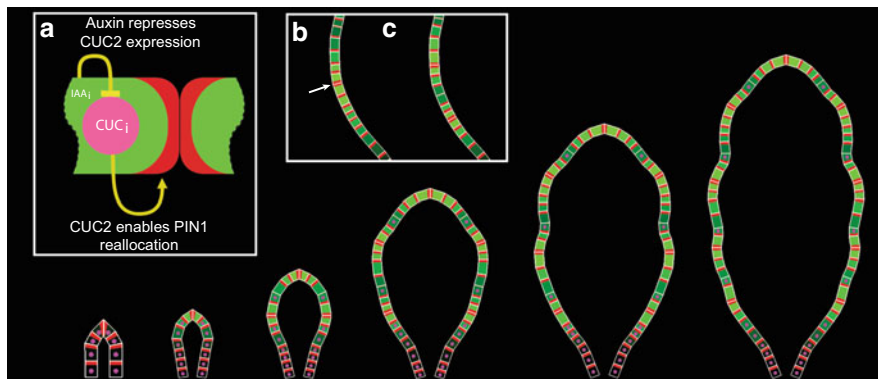
Fig. 15.11 The model of leaf margin development proposed by Bilsborough et al. (2011). Polarized PIN1 proteins are shown in *red*, cellular auxin concentrations in *green*, and CUC2 expression is indicated by the presence of *pink circles* in the center of the cells. The model assumes that PIN1 polarizes up the gradient of auxin concentration and incorporates CUC2 as the enabling factor (inset **a**). As the leaf grows, the feedback between PIN1, auxin, and CUC2 generates an interspersed pattern of auxin maxima and CUC2 expression. Increased growth at auxin maxima and growth repression at sites of CUC2 expression modulate leaf growth, producing serrations. Inset (**b**)–(**c**): a variant of the model, where PIN1 can (re)polarize in the absence of CUC2. The convergence point marked by an *arrow* in (**b**) is unstable and splits into two in (**c**). The resulting convergence points travel away from each other until a stable spacing is achieved. Figure based on Bilsborough et al. (2011)

Initial models of the initiation of leaf midveins used pure up-the-gradient (Merks et al. 2007) or with-the-flux (Stoma et al. 2008) polarization modes. These models did not fully reproduce the spatiotemporal dynamics of DR5 and PIN1 expression (Sects. 4.1 and 4.2). Bayer et al. (2009) reproduced detailed observations of leaf midvein initiation with the dual-polarization model (Sect. 4.3), which blends between both polarization modes based on auxin concentration and tissue type (Fig. 15.12). In this model, up-the-gradient polarization is dominant in the epidermis and at low auxin concentrations, whereas with-the-flux polarization is dominant in the subepidermal tissues and at high auxin concentrations. The dual-polarization model reproduces the experimentally observed spatiotemporal sequence of PIN polarizations and auxin distribution in a leaf primordium. It shows that up-the-gradient and with-the-flux polarization modes can plausibly coexist in the convergence point. It also captures the basal position of PIN proteins in the vein precursor cells, the gradual narrowing of vein-defining canals, and the towards-the-vein orientation of PINs in the cells adjacent to these canals. The model predicted a transient polarization of PIN1 proteins in the subepidermis towards the epidermis at the onset of the primordium formation. This phenomenon was subsequently observed microscopically.

While formulating their model, Bayer et al. (2009) observed that canalizing strands cannot easily find sinks representing previously formed veins. To overcome this problem, they introduced a hypothetical diffusing substance that was produced
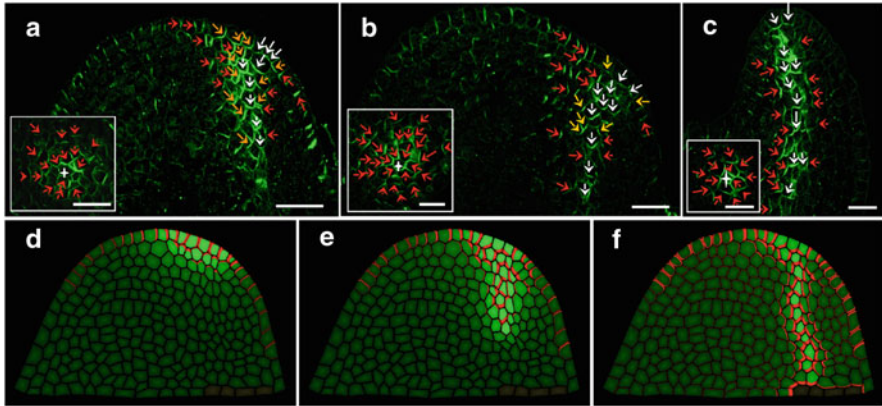
Fig. 15.12 Comparison of experimental observations with the dual model for PIN1 polarization. (**a–c**) Three stages of midvein initiation in a tomato shoot apex. Scale bars: 20 μm. *White stars* in the insets indicate the PIN1 convergence point in the L1. PIN1 immunolocalization (*green*) suggests that PINs are oriented up the gradient of auxin concentration both in the L1 and in the subepidermal tissues that surround the initiating vein (*red arrows*). In contrast, PINs at the center of the convergence point and along the midvein appear to be oriented with the auxin flux (*white arrows*). Intermediate polarities are observed at the boundary between both regions (*yellow arrows*). (**d–f**) Successive stages of a simulation of PIN polarization using the dual-polarization model. The simulation employs a cellular template approximating microscopic image (**a**). Auxin concentration is shown in *green* and PIN localization in *red*. (**d**) PINs in the inner tissue are polarized towards the convergence point forming in the epidermis. (**e**) PINs near the convergence point switch polarity as the auxin flow extends into the subepidermis. (**f**) Auxin flux reaches the sink that represents preexisting vasculature (dark cells at the bottom) and becomes refined into a narrow strand. Figure adapted from Bayer et al. (2009)

in the vasculature and polarized cells towards existing veins. The problem of finding the sink was revisited in the recent work by O'Connor et al. (2014), in the context of phyllotactic and vascular patterning in the shoot apical meristem of the grass *Brachypodium distachyon*. Confocal microscopy observations indicated that three different proteins (termed PIN1a, PIN1b, and SoPIN1—sister of PIN1) were involved in Brachypodium, in contrast to the single PIN1 in Arabidopsis. These PINs have distinct expression and cellular localization patterns, which points to differences in the mechanisms determining their polarization. Assuming that SoPIN1 proteins polarize up the gradient and the remaining two PINs polarize with the flux at different rates (linear and quadratic, respectively), O'Connor et al. modeled the observed patterns of DR5 expression and PIN localization. The model suggests that each PIN plays a distinct role. SoPIN1 generates convergence points in the epidermis. PIN1b broadly polarizes cells towards nearby vasculature, which provides a sink-finding mechanism similar to that described by Feugier et al. (2005) and Stoma et al. (2008). Finally, PIN1a canalizes broad auxin flow towards the sink into a narrow high-flux path. These results show that phyllotaxis and vascular patterning in Brachypodium can be explained by concurrent up-the-gradient and with-the-flux polarization. Their coordinated action is consistent with

the dual-polarization model. The progression from broad to canalizing auxin-driven PIN polarization suggests a mechanism for directing the emerging vein to the sink, alternative to the hypothetical factor introduced by Bayer et al. (2009).

Another model integrating up-the-gradient polarization (which leads to the emergence of convergence points) and with-the-flux polarization (which leads to the production of canals) captures the formation of the midvein and first-order laterals veins in open venation patterns, i.e., patterns without loops (Smith and Bayer 2009; Smith 2011). The model is driven by growth of the leaf blade, approximated as a single cellular layer. Questions related to the coupling of canalization and growth in the context of vein pattern formation have been highlighted and analyzed in a preliminary model study by Lee et al. (2014).

Observations by Scarpella et al. (2006) indicate that loops are formed by anastomosis, i.e., connection of canals. PIN proteins in these canals have opposite orientations, pointing away from a bipolar cell at which both canals meet. Mitchison's 1980 model and its recreation by Rolland-Lagan and Prusinkiewicz (2005) show that such a scenario of loop creation is possible if the bipolar cell is a source of auxin, turned on at a precisely defined time. A separate model of vein patterning in areoles (Dimitrov and Zucker 2006) also relies on elevated auxin concentration to localize the meeting point. However, the data of Scarpella et al. (2006) do not show an elevated auxin concentration at the meeting points. It is possible that bipolar cells are located at weak maxima of auxin concentration, not detected using experimental techniques of Scarpella et al. (2006). Another possibility, investigated using a computational model by Feugier and Iwasa (2006), is that proposed anastomosing canals are guided towards each other by a hypothetical diffusing substance. The existence of such a substance has not been experimentally confirmed. Vein pattern formation beyond the formation of the midvein and first-order lateral branches thus remains unclear.

5.4   Apical Dominance and Bud Activation

From leaves, auxin flows to the stem. There, auxin not only patterns the stem vascular system in a manner similar to the patterning of leaf veins, but also coordinates the activation of lateral buds, and thus the development of the branching structure as a whole. This coordination includes the phenomenon of apical dominance: a strong inhibitory influence of the shoot apical meristem in the vegetative state on the lateral buds below. Apical dominance is lifted upon the transition of the apex to the flowering state, resulting in the activation of one or more lateral buds in a basipetal sequence. Thimann and Skoog (1933) suggested that the inhibitory signal is auxin, produced by the shoot apex and actively transported down the plant. The use of computational models in the study of apical dominance has a particularly long history, rivaled only by Mitchison's (1980) models of auxin canalization.

The first family of models of apical dominance was created by Lindenmayer and his collaborators (Lindenmayer 1984; Janssen and Lindenmayer 1987; Prusinkiewicz et al. 1988; Prusinkiewicz and Lindenmayer 1990). The models aimed at elucidating the dynamics of branch initiation and flowering in compound inflorescences, using the herbaceous plant *Mycelis muralis* as a case study. To switch apical meristems in the main and lateral branches from the vegetative to flowering state, the models incorporated an additional long-distance signal, representing a then hypothetical flower-inducing substance, "florigen." The nature of florigen has since then been established (Lifschitz et al. 2006; Lifschitz and Eshed 2006; Shalit et al. 2009; Zeevaart 2008), opening the door for future models that may lead to a deeper understanding of inflorescence development.

Lindenmayer and his collaborators hypothesized that the timing of activation of successive buds reflects the speed with which the wave of auxin depletion propagates down the stem after the transition of the apical meristem to flowering. This hypothesis put in focus several questions. First, it is not clear how the resulting models could account for the activation sequences of buds within rosettes. There, extremely short internodes should lead to almost simultaneous activation of lateral buds, yet in Arabidopsis, for example, a basipetal sequence is observed in the rosette in spite of the short internodes (Stirnberg et al. 1999). Second, the depletion-wave models do not take into consideration contributions of the lateral branches to the auxin flow in the stem, contrary to experimental data (Morris 1977). Third, experiments with radiolabeled auxin show that auxin transported from the main apex through the stem does not pass in the vicinity of the dormant buds and does not enter them (Morris 1977). It is thus not clear how the auxin signal is conveyed to the bud. One possibility is that auxin acts on the lateral bud indirectly, through the intermediacy of one or more other hormones that move freely between the stem and the bud and act as secondary messengers. Candidate hormones are cytokinin (Muüller and Leyser 2011; Shimizu-Sato et al. 2008) and strigolactone (Gomez-Roldan et al. 2008; Dun et al. 2009; Brewer et al. 2009; Agusti et al. 2011), possibly acting jointly (Dun et al. 2012). Modeling shows, however, that this intermediacy is not necessary, and all three shortcomings of the auxin-depletion model can be addressed with a "relay" model using only auxin (Prusinkiewicz et al. 2009; Leyser 2009; Shinohara et al. 2013).

The relay model is based on the assumption, most recently supported by Furutani et al. (2014), that a lateral bud remains dormant until it can effectively export the auxin it produces through a polar transport mechanism. Bifurcation analysis of the with-the-flux model of auxin transport (Prusinkiewicz et al. 2009) shows that such export can be triggered by a temporary decrease of auxin concentration in the stem segment (metamer) supporting the bud, which the bud senses through an increase in the background auxin flow from the bud. Once triggered, the polar auxin transport is maintained even after the high level of auxin concentration in the metamer is restored by the auxin efflux from the activated bud.

In the context of a branched shoot, the temporary decrease of auxin concentration in a metamer results from a decrease in auxin supply from the shoot apical meristem and/or lateral meristems positioned further up the stem. A more basipetal
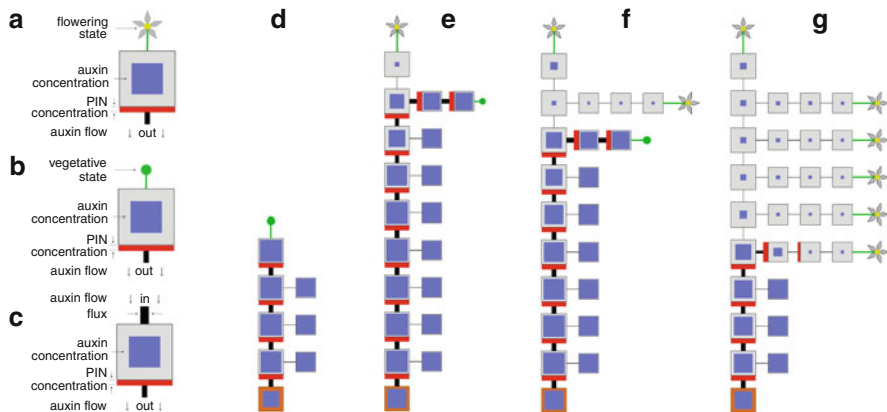
Fig. 15.13 The relay model of bud activation at the metamer level. (**a**, **b**) Schematic representations of an apex in the flowering and vegetative state. (**c**) Representation of a metamer. (**d–g**) Selected stages of the simulation. At the beginning of the simulation, the main apex creates a sequence of metamers with the associated lateral buds. Due to the high supply of auxin from the apex, the concentration of auxin in the metamers is high (**d**). Upon transition to flowering, production of auxin in the main apex decreases, causing a decrease in auxin concentration in the stem. This decrease is the strongest in the topmost metamer, triggering polar auxin efflux from the associated lateral bud that activates it. Auxin produced by this bud re-saturates the stem (**e**). After transition of the topmost bud to the flowering state, next lateral bud becomes activated (**f**). The resulting relay process continues (**g**) until all buds have become activated. Figure based on Prusinkiewicz et al. (2009)

bud is thus activated when the bud higher up switches from the vegetative to the flowering state. By the same mechanism, the subsequent switch to flowering of the most recently activated bud triggers activation of the next one, and the relay progresses (Fig. 15.13). In contrast to the depletion model, the timing of this progression is determined by the delay between the activation of a lateral bud and its switch to flowering. Auxin propagation times thus play a secondary role.

The relay model extrapolates the with-the-flux auxin polarization model from the level of individual cells to the level of architectural modules of a plant: apices, buds, and metamers. An important aspect of with-the-flux polarization is its ability to canalize auxin flow into narrow streams, precursors of vascular strands (Fig. 15.7c). In the case of lateral buds, vascular connections may be formed concurrently with, and indeed as an integral part of, increased auxin outflow from the buds (Grbic and Bleecker 2000). A cellular-level version of the relay model (Fig. 15.14) shows that it is compatible with such a behavior.

The secondary messenger model and the model explaining apical dominance and bud activation in terms of the properties of with-the-flux polarization are not mutually exclusive. As the mechanisms of apical control continue to be actively studied, the use of models elucidating logical consequences of different assumptions fulfills one of key roles of modeling: to sharpen the questions.
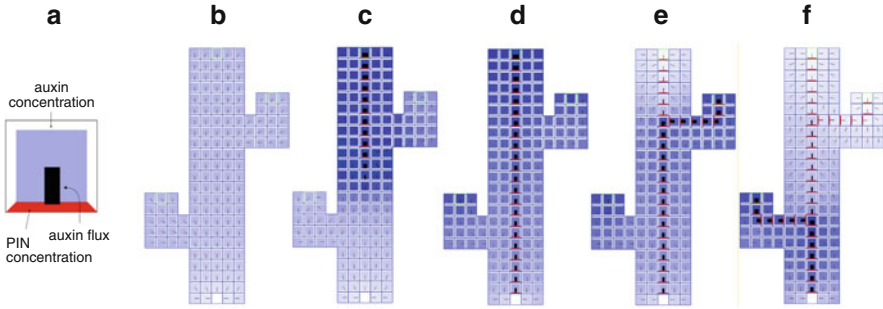
Fig. 15.14 The relay model of bud activation at the cellular level. The cellular grid represents a longitudinal section of a stem with two buds. (**a**) Iconic representation of a cell. (**b–f**) Selected stages of the simulation. Following the placement of an auxin source at the top of the main segment, a vascular strand running through the segment emerges (**c**). Subsequent placement of auxin sources in the two buds (**d**) does not trigger formation of lateral vasculature until the auxin source at the top of the main stem is deactivated. The resulting decrease of auxin concentration in the main vasculature then triggers the formation of a vein connecting the higher bud to the central vasculature (**e**). When the source of auxin associated with this bud is deactivated, a similar process occurs in the lower bud (**f**). Figure adapted from Prusinkiewicz et al. (2009)

5.5   Root Development

As described by the reverse/inverse fountain model (Fig. 15.1), auxin from the stem flows into the root. There, PINs are localized towards the root apex in the vasculature and away from it in the epidermis and cortex. Consistent with these localizations, auxin flows towards the root apex in the subepidermal layers and away from it in the epidermis. In the outer layers PIN proteins are also partially polarized towards the central axis of the root. As a result, auxin from the outer layers reenters the inner layers and is recycled towards the root tip. This recycling underlies the maintenance of an auxin maximum at the root apex. Grieneisen et al. (2007) capture this phenomenon using a model operating on a static grid and a model incorporating growth and division of approximately rectangular cells. In both cases PIN polarities were predefined. Similar spatial patterns of auxin concentration were subsequently obtained by Santuari et al. (2011), who used static cellular templates based on digitized microscopy images (Fig. 15.15). Cellular templates were also used by Stoma et al. (2008), who assumed that PINs are polarized according to the with-the-flux model. They showed that auxin maxima are maintained in this case as well.

In contrast to the above models, which were focused on the maintenance of the auxin maximum at the root tip, Mironova et al. (2010) addressed the problem of the emergence of this maximum and its regeneration after the removal of the root tip. They modeled these phenomena by assuming that PINs in different root layers have predefined polarizations, but their concentrations depend on the concentration of auxin. Mironova et al. (2012) extended that model by incorporating three different PIN proteins, PIN1, PIN2, and PIN3, and assuming that their expression and turnover rates respond differently to auxin concentration levels.
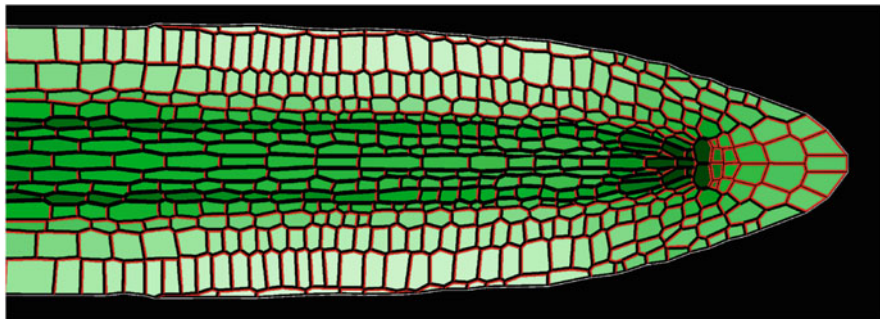
Fig. 15.15 A model of auxin fluxes in the root. PINs (*red*) polarize towards the root tip in the central vascular system and away from the tip in the epidermis and cortex. Note the presence of PINs directing auxin back into the vasculature in the outer cell layers. This causes a reflux of auxin (*green*) back to the tip, allowing the system to store auxin even after the shoot is removed (Grieneisen et al. 2007). Simulation adapted from Santuari et al. (2011)

Grieneisen et al. (2007) used their model to propose that the recycling ("reflux") of auxin at the root tip produces an "auxin capacitor," where auxin is gradually accumulated. An extension of this idea underlies the mechanistic models of lateral root initiation proposed by Lucas et al. (2008a, b). In these models, the auxin capacitor at the root tip is charged by the basipetal flux of auxin. The capacitor is periodically discharged when the auxin level exceeds a threshold. The discharge triggers the formation of a lateral root. The models explain the timing of the initiation of lateral roots. Although they do not have a spatial character, they yield a spatial distribution of lateral roots when a rate of main root growth is assumed.

Fortin et al. (1989) observed that the sites of lateral root initiation are primed by root geometry, as lateral roots tend to form on the convex side of a curved main root. Investigating this phenomenon with computational models, Laskowski et al. (2008) found that longer cells on the convex side accumulate more auxin than shorter cells on the concave side. These differences are amplified by the auxin-dependent upregulation of auxin transport to cells by the AUX1 proteins. The higher auxin concentration on the convex side prompts preferential establishment of auxin maxima on the same side. These maxima induce lateral roots (Benková et al. 2003).

The model by Laskowski et al. (2008) showed that a feedback between auxin and its importers may play a role in auxin-driven patterning. As shown in Sect. 4.4, such a feedback can theoretically create a pattern of approximately equidistant auxin maxima even in the absence of the more widely considered feedback between auxin and its exporters.

6   Conclusions

Computational modeling of auxin-driven patterning got off to an early start with
Mitchison's (1980) exploration of Sachs's canalization theory (Sachs 1969), but for
the next 25 years the area remained dormant. The situation changed in the early
2000s with the explosion of new experimental techniques. Immunological detection
(Sauer and Friml 2010) and fluorescent tagging (Millar et al. 2009) have made it
possible to display the localization patterns of proteins in different tissues at
subcellular resolution. In vivo techniques (Heisler et al. 2005) enabled the obser-
vation of these localizations over time. Genetic manipulations led to remarkable
advancements in the study of protein functions. The experimental results prompted
by these techniques have led to new hypotheses regarding mechanisms of pattern
formation in plants. Computational models turned out to be useful in testing
whether these hypotheses are plausible. They also put into focus many crucial
questions, in particular regarding the biological mechanisms of PIN polarization
(Bennett et al. 2013), which are subject of current research.

In contrast to the experimental systems, where causal relations are not directly
observed, in computational models such relations are explicitly assumed. This
makes models indispensable, as they provide the only rigorous means to examine
whether proposed mechanisms can indeed yield the observed patterns and forms.
The use of computational models for this purpose began with the examination
(Jönsson et al. 2006; Smith et al. 2006a; Barbier de Reuille et al. 2006) of the
conceptual model of phyllotaxis introduced by Reinhardt et al. (2003). Models
examining further auxin-driven processes in plants, including apical control and the
development of leaves and roots, quickly followed (Sect. 5). Extensions to other
processes and systems (e.g., regulation of embryonic development and mediation of
tropic responses in plants) are forthcoming.

In addition to explaining phenomena based on experimental data, computational
models highlight areas where experimental data are insufficient. At present, one
such area encompasses molecular mechanisms of PIN polarization. Models exam-
ining different hypothetical mechanisms have been proposed (Sect. 4.5), but data
that would put them on a solid experimental foundation are still not available. Their
theoretical implications and relations to the higher-level up-the-gradient, with-the-
flux, and dual-polarization models also require a better understanding. This is
needed to connect models operating at different scales and levels of abstraction
(Fig. 15.2). An intriguing element of the puzzle is the extent to which the interplay
between mechanical stresses and the distribution of auxin transporters (Hamant
et al. 2008; Hamant and Traas 2010; Boudaoud 2010; Heisler et al. 2010), as well as
growth, may play a role in PIN polarization and the resulting regulation of devel-
opment. Furthermore, production of leaves and vascular systems in *pin* mutants
(Barkoulas et al. 2008; Bilsborough et al. 2011) indicate that the feedback between
PIN proteins and polar auxin transport represents only one facet of the relevant
patterning processes (Guenot et al. 2012; Kierzkowski et al. 2013). Problems of
current interest also concern the interplay between auxin and other substances (e.g.,

cytokinin, strigolactone) and the role of auxin synthesis in patterning. Furthermore, mechanistic links between auxin-related patterns and the resulting macroscopic forms, for example, the diverse forms of leaves, remain an area of active study.

From the methodological perspective, most models of auxin-driven patterning and growth devised to date operate on surfaces. In some cases, however, the use of three-dimensional models appears to be essential. One example is the modeling of vascular pattern development in stems. The methodology for creating and visualizing three-dimensional models, especially those operating on growing tissues as opposed to static templates, is yet to be fully developed.

References

Abley K, Barbier de Reuille P, Strutt D, Bangham A, Prusinkiewicz P, Marée A, Grieneisen V, Coen E (2013) An intracellular partitioning-based framework for tissue cell polarity in plants and animals. Development 140(10):2061–2074

Agusti J, Herold S, Schwarz M, Sanchez P, Ljung K, Dun E, Brewer P, Beveridge C, Sieberer T, Sehr E, Greb T (2011) Strigolactone signaling is required for auxin-dependent stimulation of secondary growth in plants. Proc Natl Acad Sci U S A 108(50):20242–20247

Arber A (1950) The natural philosophy of plant form. University Press, Cambridge

Bainbridge K, Guyomarc'h S, Bayer E, Swarup R, Bennett M, Mandel T, Kuhlemeier C (2008) Auxin influx carriers stabilize phyllotactic patterning. Genes Dev 22(6):810–823

Banasiak A (2011) Putative dual pathway of auxin transport in organogenesis of *Arabidopsis*. Planta 233(1):49–61

Barbier de Reuille P, Bohn-Courseau I, Ljung K, Morin H, Carraro N, Godin C, Traas J (2006) Computer simulations reveal properties of the cell-cell signaling network at the shoot apex in *Arabidopsis*. Proc Natl Acad Sci U S A 103(5):1627–1632

Barkoulas M, Hay A, Kougioumoutzi E, Tsiantis M (2008) A developmental framework for dissected leaf formation in the *Arabidopsis* relative *Cardamine hirsuta*. Nat Genet 40 (9):1136–1141

Bayer E, Smith R, Mandel T, Nakayama N, Sauer M, Prusinkiewicz P, Kuhlemeier C (2009) Integration of transport-based models for phyllotaxis and midvein formation. Genes Dev 23 (3):373–384

Ben-Gera H, Shwartz I, Shao M, Shani E, Estelle M, Ori N (2012) ENTIRE and GOBLET promote leaflet development in tomato by modulating auxin response. Plant J 70(6):903–915

Benková E, Michniewicz M, Sauer M, Teichmann T, Seifertova D, Jürgens G, Friml J (2003) Local, efflux-dependent auxin gradients as a common module for plant organ formation. Cell 115(5):591–602

Bennett M, Marchant A, Green H, May S, Ward S, Millner P, Walker A, Schulz B, Feldmann K (1996) Arabidopsis AUX1 gene: a permease-like regulator of root gravitropism. Science 273 (5277):948–950

Bennett T, Sieberer T, Willett B, Booker J, Luschnig C, Leyser O (2006) The Arabidopsis MAX pathway controls shoot branching by regulating auxin transport. Curr Biol 16(6):553–563

Bennett T, Hines G, Leyser O (2013) Canalization: what the flux? Trends Genet 30(2):41–48

Berger Y, Harpaz-Saad S, Brand A, Melnik H, Sirding N, Alvarez J, Zinder M, Samach A, Eshed Y, Ori N (2009) The NAC-domain transcription factor GOBLET specifies leaflet boundaries in compound tomato leaves. Development 136(5):823–832

Berleth T, Scarpella E, Prusinkiewicz P (2007) Towards the systems biology of auxin-transport-mediated patterning. Trends Plant Sci 12(14):151–159

Besnard F, Refahi Y, Morin V, Marteaux B, Brunoud G, Chambrier P, Rozier F, Mirabet V, Legrand J, Lainé S, Thévenon E, Farcot E, Cellier C, Das P, Bishopp A, Dumas R, Parcy F, Helariutta Y, Boudaoud A, Godin C, Traas J, Guédon Y, Vernoux T (2014) Cytokinin signalling inhibitory fields provide robustness to phyllotaxis. Nature 505:417–421

Besson S, Dumais J (2011) Universal rule for the symmetric division of plant cells. Proc Natl Acad Sci U S A 108(15):6294–6299

Bilsborough G, Runions A, Barkoulas M, Jenkins H, Hasson A, Galinha C, Laufs P, Hay A, Prusinkiewicz P, Tsiantis M (2011) Model for the regulation of *Arabidopsis thaliana* leaf margin development. Proc Natl Acad Sci U S A 108(8):3424–3429

Boudaoud A (2010) An introduction to the mechanics of morphogenesis for plant biologists. Trends Plant Sci 15(6):353–360

Brewer P, Dun E, Ferguson B, Rameau C, Beveridge C (2009) Strigolactone acts downstream of auxin to regulate bud outgrowth in pea and *Arabidopsis*. Plant Physiol 150(1):482–493

Camazine S, Deneubourg J, Franks N, Sneyd J, Theraulaz G, Bonabeau E (2001) Self-organization in biological systems. Princeton University Press, Princeton, NJ

Champagne C, Sinha N (2004) Compound leaves: equal to the sum of their parts? Development 131(18):4401–4412

Chitwood D, Headland L, Ranjan A, Martinez C, Braybrook S, Koenig D, Kuhlemeier C, Smith R, Sinha N (2012) Leaf asymmetry as a developmental constraint imposed by auxin-dependent phyllotactic patterning. Plant Cell 24(16):2318–2327

Corson F, Adda-Bedia M, Boudaoud A (2009) In silico leaf venation networks: growth and reorganization driven by mechanical forces. J Theor Biol 259(3):440–448

Couder Y, Pauchard L, Allain C, Adda-Bedia M, Douady S (2002) The leaf venation as formed in a tensorial field. Eur Phys J B Condens Matter Complex Syst 28(2):135–138

Crawford S, Shinohara N, Sieberer T, Williamson L, George G, Hepworth J, Muller D, Domagalska M, Leyser O (2010) Strigolactones enhance competition between shoot branches by dampening auxin transport. Development 137(17):2905–2913

Dimitrov P, Zucker S (2006) A constant production hypothesis guides leaf venation patterning. Proc Natl Acad Sci U S A 103(24):9363–9368

Draelants D, Broeckhove J, Beemster G, Vanroose W (2012) Numerical bifurcation analysis of the pattern formation in a cell based auxin transport model. J Math Biol 67(5):1279–1305

Dun E, Brewer P, Beveridge C (2009) Strigolactones: discovery of the elusive shoot branching hormone. Trends Plant Sci 14(7):364–372

Dun E, de Saint Germain A, Rameau C, Beveridge C (2012) Antagonistic action of strigolactone and cytokinin in bud outgrowth control. Plant Physiol 158(1):487–498

Edmonds J (1960) A combinatorial representation for polyhedral surfaces. Notices Amer Math Soc 7:646

Errera L (1886) Sur une condition fondamentale d'équilibre des cellules vivantes. Comptes Rendus Hebdomadaires des Seances de l'Academie des Sciences 103:822–824

Fan Y, Litven J, Levin D, Pai D (2013) Eulerian-on-Lagrangian simulation. ACM Trans Graph 32 (3):22:1–22:9

Farcot E, Yuan Y (2013) Homogenous auxin steady states and spontaneous oscillations in flux-based auxin transport models. SIAM J Appl Dyn Syst 12(3):1330–1353

Feugier F, Iwasa Y (2006) How canalization can make loops: a new model of reticulated leaf vascular pattern formation. J Theor Biol 243(2):235–244

Feugier F, Mochizuki A, Iwasa Y (2005) Self-organization of the vascular system in plant leaves: inter-dependent dynamics of auxin flux and carrier proteins. J Theor Biol 236(4):366–375

Fortin M, Pierce F, Poff K (1989) The pattern of secondary root formation in curving roots of *Arabidopsis thaliana* (L.) Heynh. Plant Cell Environ 12(3):337–339

Fozard J, King J, Bennett M (2013) Modelling auxin efflux carrier phosphorylation and localization. J Theor Biol 319:34–49

Friml J, Yang X, Michniewicz M, Weijers D, Quint A, Tietz O, Benjamins R, Ouwerkerk P, Ljung K, Sandberg G, Hooykaas P, Palme K, Offringa R (2004) A PINOID-dependent binary switch in apical-basal PIN polar targeting directs auxin efflux. Science 306(5697):862–865

Fujita H, Mochizuki A (2006) Pattern formation of leaf veins by the positive feedback regulation between auxin flow and auxin efflux carrier. J Theor Biol 241(3):541–551

Furutani M, Nakano Y, Tasaka M (2014) MAB4-induced auxin sink generates local auxin gradients in *Arabidopsis* organ formation. Proc Natl Acad Sci U S A 111(3):1198–1203

Garnett P, Stepney S, Leyser O (2008) Towards an executable model of auxin transport canalisation. In: Stepney S, Polack F, Welch P (eds) Proceedings of the 2008 workshop on complex systems modelling and simulation. Luniver Press, Frome, pp 63–91

Geldner N, Friml J, Stierhof Y, Jürgens G, Palme K (2001) Auxin transport inhibitors block PIN1 cycling and vesicle trafficking. Nature 413(6854):425–428

Gillespie D (1976) A general method for numerically simulating the stochastic time evolution of coupled chemical reactions. J Comput Phys 22(4):403–434

Gillespie D (1977) Exact stochastic simulation of coupled chemical reactions. J Phys Chem 81(25):2340–2361

Goldsmith M (1977) The polar transport of auxin. Annu Rev Plant Physiol 28:439–478

Gomez-Roldan V, Fermas S, Brewer P, Puech-Pages V, Dun E, Pillot J, Letisse F, Matusova R, Danoun S, Portais J, Bouwmeester H, Bécard G, Beveridge C, Rameau C, Rochange S (2008) Strigolactone inhibition of shoot branching. Nature 455(7210):189–194

Grbic V, Bleecker AB (2000) Axillary meristem development in *Arabidopsis thaliana*. Plant J 21(2):215–223

Grieneisen V, Xu J, Marée A, Hogeweg P, Scheres B (2007) Auxin transport is sufficient to generate a maximum and gradient guiding root growth. Nature 449(7165):1008–1013

Guenot B, Bayer E, Kierzkowski D, Smith R, Mandel T, Zadnikova P, Benková E, Kuhlemeier C (2012) PIN1-independent leaf initiation in Arabidopsis. Plant Physiol 159(4):1501–1510

Hamant O, Traas J (2010) The mechanics behind plant development. New Phytol 185(2):369–385

Hamant O, Heisler M, Jönsson H, Krupinski P, Uyttewaal M, Bokov P, Corson F, Sahlin P, Boudaoud A, Meyerowitz E, Couder Y, Traas J (2008) Developmental patterning by mechanical signals in *Arabidopsis*. Science 322(5908):1650–1655

Hay A, Barkoulas M, Tsiantis M (2006) ASYMMETRIC LEAVES1 and auxin activities converge to repress *BREVIPEDICELLUS* expression and promote leaf development in *Arabidopsis*. Development 133(20):3955–3961

Heisler M, Jönsson H (2006) Modeling auxin transport and plant development. J Plant Growth Regul 25(4):302–312

Heisler M, Ohno C, Das P, Sieber P, Reddy G, Long J, Meyerowitz E (2005) Patterns of auxin transport and gene expression during primordium development revealed by live imaging of the Arabidopsis inflorescence meristem. Curr Biol 15(21):1899–1911

Heisler M, Hamant O, Krupinski P, Uyttewaal M, Ohno C, Jönsson H, Traas J, Meyerowitz E (2010) Alignment between PIN1 polarity and microtubule orientation in the shoot apical meristem reveals a tight coupling between morphogenesis and auxin transport. PLoS Biol 8(10):e1000516

Hofmeister W (1868) Allgemeine Morphologie der Gewachse. Engelmann, Leipzig, pp 405–664

Hošek P, Kubes M, Lankova M, Dobrev P, Klima P, Kohoutova M, Petrasek J, Hoyerova K, Jirina M, Zažímalová E (2012) Auxin transport at cellular level: new insights supported by mathematical modelling. J Exp Bot 63(10):3815–3827

Janssen J, Lindenmayer A (1987) Models for the control of branch positions and flowering sequences of capitula in *Mycelis muralis* (L.) Dumont (Compositae). New Phytol 105(2):191–220

Jönsson H, Heisler M, Shapiro B, Meyerowitz E, Mjolsness E (2006) An auxin-driven polarized transport model for phyllotaxis. Proc Natl Acad Sci U S A 103(5):1633–1638

Kawamura E, Horiguchi G, Tsukaya H (2010) Mechanisms of leaf tooth formation in *Arabidopsis*. Plant J 62(3):429–441

Kierzkowski D, Lenhard M, Smith R, Kuhlemeier C (2013) Interaction between meristem tissue layers controls phyllotaxis. Dev Cell 26(6):616–628

Koenig D, Bayer E, Kang J, Kuhlemeier C, Sinha N (2009) Auxin patterns *Solanum lycopersicua*m leaf morphogenesis. Development 136(17):2997–3006

Kramer E (2004) PIN and AUX/LAX proteins: their role in auxin accumulation. Trends Plant Sci 9 (12):578–582

Kramer E (2009) Auxin-regulated cell polarity: an inside job? Trends Plant Sci 14(5):242–247

Laguna M, Bohn S, Jagla E (2008) The role of elastic stresses on leaf venation morphogenesis. PLoS Comput Biol 4(4):e1000055

Larson P (1975) Development and organization of the primary vascular system in *Populus deltoides* according to phyllotaxy. Am J Bot 62(10):1084–1099

Laskowski M, Biller S, Stanley K, Kajstura T, Prusty R (2006) Expression profiling of auxin-treated *Arabidopsis* roots: toward a molecular analysis of lateral root emergence. Plant Cell Physiol 47(6):788–792

Laskowski M, Grieneisen V, Hofhuis H, ten Hove C, Hogeweg P, Marée A, Scheres B (2008) Root system architecture from coupling cell shape to auxin transport. PLoS Biol 6(12):e307

Lee S-W, Feugier F, Morishita Y (2014) Canalization-based vein formation in a growing leaf. J Theor Biol 353C:104–120

Leyser O (2009) The control of shoot branching: an example of plant information processing. Plant Cell Environ 32(6):694–703

Leyser O (2011) Auxin, self-organization, and the colonial nature of plants. Curr Biol 21(9):R331–R337

Lifschitz E, Eshed Y (2006) Universal florigenic signals triggered by FT homologues regulate growth and flowering cycles in perennial day-neutral tomato. J Exp Bot 57(13):3405–3414

Lifschitz E, Eviatar T, Rozman A, Shalit A, Goldshmidt A, Amsellem Z, Alvarez J, Eshed Y (2006) The tomato FT ortholog triggers systemic signals that regulate growth and flowering and substitute for diverse environmental stimuli. Proc Natl Acad Sci U S A 103(16):6398–6403

Lindenmayer A (1984) Positional and temporal control mechanisms in inflorescence development. In: Barlow PW, Carr DJ (eds) Positional controls in plant development. University Press, Cambridge, pp 461–486

Lockhart J (1965) An analysis of irreversible plant cell elongation. J Theor Biol 8(2):264–275

Lucas M, Godin C, Jay-Allemand C, Laplaze L (2008a) Auxin fluxes in the root apex coregulate gravitropism and lateral root initiation. J Exp Bot 59(1):55–66

Lucas M, Guédon Y, Jay-Allemand C, Godin C, Laplaze L (2008b) An auxin transport-based model of root branching in *Arabidopsis thaliana*. PLoS One 3(11):e3673

Marhavý P, Bielach A, Abas L, Abuzeineh A, Duclercq J, Tanaka H, Parežová M, Petrášek J, Friml J, Kleine-Vehn J, Benková E (2011) Cytokinin modulates endocytic trafficking of PIN1 auxin efflux carrier to control plant organogenesis. Dev Cell 21(4):796–804

Meinhardt H (1982) Models of biological pattern formation. Academic, London

Merks R, Glazier J (2005) A cell-centered approach to developmental biology. Phys A 352:113–130

Merks R, Van de Peer Y, Inzé D, Beemster G (2007) Canalization without flux sensors: a traveling-wave hypothesis. Trends Plant Sci 12(9):384–390

Merks R, Guravage M, Inzé D, Beemster G (2011) VirtualLeaf: an open-source framework for cell-based modeling of plant tissue growth and development. Plant Physiol 155(2):656–666

Millar A, Carrie C, Pogson B, Whelan J (2009) Exploring the function-location nexus: using multiple lines of evidence in defining the subcellular location of plant proteins. Plant Cell 21 (6):1625–1631

Mirabet V, Besnard F, Vernoux T, Boudaoud A (2012) Noise and robustness in phyllotaxis. PLoS Comput Biol 8(2):e1002389

Mironova V, Omelyanchuk N, Yosiphon G, Fadeev S, Kolchanov N, Mjolsness E, Likhoshvai V (2010) A plausible mechanism for auxin patterning along the developing root. BMC Syst Biol 4(98):1–19

Mironova V, Omelyanchuk N, Novoselova E, Doroshkov A, Kazantsev F, Kochetov A, Kolchanov N, Mjolsness E, Likhoshvai V (2012) Combined in silico/in vivo analysis of mechanisms providing for root apical meristem self-organization and maintenance. Ann Bot 110(2):349–360

Mitchison G (1980) A model for vein formation in higher plants. Proc R Soc B 207:79–109

Mitchison G (1981) The polar transport of auxin and vein patterns in plants. Philos Trans Roy Soc Lond B 295:461–470

Moreno-Risueno M, Van Norman J, Moreno A, Zhang J, Ahnert S, Benfey P (2010) Oscillating gene expression determines competence for periodic Arabidopsis root branching. Science 329 (5997):1306–1311

Morris D (1977) Transport of exogenous auxin in two-branched dwarf pea seedlings (*Pisum sativum* L.). Planta 136(1):91–96

Muller D, Leyser O (2011) Auxin, cytokinin and the control of shoot branching. Ann Bot 107 (7):1203–1212

Napier R, David K, Perrot-Rechenmann C (2002) A short history of auxin-binding proteins. Plant Mol Biol 49(3–4):339–348

Nikovics K, Blein T, Peaucelle A, Ishida T, Morin H, Aida M, Laufs P (2006) The balance between the MIR164A and CUC2 genes controls leaf margin serration in *Arabidopsis*. Plant Cell 18(11):2929–2945

O'Connor D, Runions A, Sluis A, Bragg J, Vogel J, Prusinkiewicz P, Hake S (2014) A division in PIN-mediated patterning during lateral organ initiation in the grasses. PLoS Comput Biol 10 (1):e1003447

Paciorek T, Zažímalová E, Ruthardt N, Petrasek J, Stierhof Y, Kleine-Vehn J, Morris D, Emans N, Jürgens G, Geldner N, Friml J (2005) Auxin inhibits endocytosis and promotes its own efflux from cells. Nature 435(7046):1251–1256

Paponov I, Paponov M, Teale W, Menges M, Chakrabortee S, Murray J, Palme K (2008) Comprehensive transcriptome analysis of auxin responses in *Arabidopsis*. Mol Plant 1 (2):321–337

Parry G, Marchant A, May S, Swarup R, Swarup K, James N, Graham N, Allen T, Martucci T, Yemm A, Napier R, Manning K, King G, Bennett M (2001) Quick on the uptake: characterization of a family of plant auxin influx carriers. J Plant Growth Regul 20(30):217–225

Pinon V, Prasad K, Grigg S, Sanchez-Perez G, Scheres B (2013) Local auxin biosynthesis regulation by PLETHORA transcription factors controls phyllotaxis in *Arabidopsis*. Proc Natl Acad Sci U S A 110(3):1107–1112

Prusinkiewicz P, Lindenmayer A (1990) The algorithmic beauty of plants. Springer, New York, NY. With JS Hanan, FD Fracchia, DR Fowler, MJM de Boer, and L Mercer

Prusinkiewicz P, Runions A (2012) Computational models of plant form and development. New Phytol 193(3):549–569

Prusinkiewicz P, Lindenmayer A, Hanan J (1988) Developmental models of herbaceous plants for computer imagery purposes. Comput Graph 22:141–150

Prusinkiewicz P, Crawford S, Smith R, Ljung K, Bennett T, Ongaro V, Leyser O (2009) Control of bud activation by an auxin transport switch. Proc Natl Acad Sci U S A 106(41):17431–17436

Raven J (1975) Transport of indoleacetic acid in plant cells in relation to pH and electrical potential gradients, and its significance for polar IAA transport. New Phytol 74(2):163–172

Reinhardt D, Pesce E, Stieger P, Mandel T, Baltensperger K, Bennett M, Traas J, Friml J, Kuhlemeier C (2003) Regulation of phyllotaxis by polar auxin transport. Nature 426 (6964):255–260

Renton M, Hanan J, Ferguson B, Beveridge C (2012) Models of long-distance transport: how is carrier-dependent auxin transport regulated in the stem? New Phytol 194(3):704–715

Robert S, Kleine-Vehn J, Barbez E, Sauer M, Paciorek T, Baster P, Vanneste S, Zhang J, Simon S, Covanova M, Hayashi K, Dhonukshe P, Yang Z, Bednarek S, Jones A, Luschnig C, Anieto F, Zažímalová E, Friml J (2010) ABP1 mediates auxin inhibition of clathrin-dependent endocytosis in *Arabidopsis*. Cell 143(1):111–121

Rolland-Lagan A, Prusinkiewicz P (2005) Reviewing models of auxin canalization in the context of leaf vein pattern formation in *Arabidopsis*. Plant J 44(5):854–865

Roussel M, Slingerland M (2012) A biochemically semi-detailed model of auxin-mediated vein formation in plant leaves. BioSyst 109(3):475–487

Rubery P, Sheldrake R (1974) Carrier-mediated auxin transport. Planta 118:101–121

Rutschow H, Baskin T, Kramer E (2011) Regulation of solute flux through plasmodesmata in the root meristem. Plant Physiol 155(4):1817–1826

Sachs T (1969) Polarity and the induction of organized vascular tissues. Ann Bot 33(2):263–275

Sachs T (1981) The control of patterned differentiation of vascular tissues. Adv Bot Res 9:151–262

Sachs T (1991) Pattern formation in plant tissues. Cambridge University Press, Cambridge

Sachs T (2003) Collective specification of cellular development. Bioessays 25(9):897–903

Sahlin P, Söderberg B, Jönsson H (2009) Regulated transport as a mechanism for pattern generation: capabilities for phyllotaxis and beyond. J Theor Biol 258(1):60–70

Santuari L, Scacchi E, Rodriguez-Villalon A, Salinas P, Dohmann E, Brunoud G, Vernoux T, Smith R, Hardtke C (2011) Positional information by differential endocytosis splits auxin response to drive Arabidopsis root meristem growth. Curr Biol 21(22):1918–1923

Sauer M, Friml J (2010) Immunolocalization of proteins in plants. In: Hennig L, Köhler C (eds) Plant developmental biology: methods ad protocols. Humana, New York, NY, pp 253–263

Scarpella E, Marcos D, Friml J, Berleth T (2006) Control of leaf vascular patterning by polar auxin transport. Genes Dev 20(8):1015–1027

Shalit A, Rozman A, Goldshmidt A, Alvarez J, Bowman J, Eshed Y, Lifschitz E (2009) The flowering hormone florigen functions as a general systemic regulator of growth and termination. Proc Natl Acad Sci U S A 106(20):8392–8397

Shapiro B, Meyerowitz E, Mjolsness E (2013) Using Cellzilla for plant growth simulations at the cellular level. Front Plant Sci 4(408):1–9

Shimizu-Sato S, Tanaka M, Mori H (2008) Auxin–cytokinin interactions in the control of shoot branching. Plant Mol Biol 69(4):429–435

Shinohara N, Taylor C, Leyser O (2013) Strigolactone can promote or inhibit shoot branching by triggering rapid depletion of the auxin efflux protein PIN1 from the plasma membrane. PLoS Biol 11(1):e1001474

Smith C (2006) On vertex-vertex systems and their use in geometric and biological modelling. PhD Thesis, University of Calgary, Calgary

Smith R (2011) Modeling plant morphogenesis and growth. In: Amar M, Goriely A, Mueller M, Cugliandolo L (eds) New trends in the physics and mechanics of biological systems, vol 92, Lecture notes of the Les Houches summer school, July 2009. Oxford University Press, Oxford, pp 301–336

Smith R, Bayer E (2009) Auxin transport-feedback models of patterning in plants. Plant Cell Environ 32(5):1258–1271

Smith C, Prusinkiewicz P, Samavati F (2004) Local specification of subdivision algorithms. In: Pfaltz J (ed) Applications of graph transformations with industrial relevance, vol 3062, Lecture notes in computer science. Springer, Berlin, pp 313–327

Smith R, Guyomarc'h S, Mandel T, Reinhardt D, Kuhlemeier C, Prusinkiewicz P (2006a) A plausible model of phyllotaxis. Proc Natl Acad Sci U S A 103:1301–1306

Smith R, Kuhlemeier C, Prusinkiewicz P (2006b) Inhibition fields for phyllotactic pattern formation: a simulation study. Can J Bot 84:1635–1649

Steinacher A, Leyser O, Clayton R (2012) A computational model of auxin and pH dynamics in a single plant cell. J Theor Biol 296:84–94

Stirnberg P, Chatfield S, Leyser O (1999) AXR1 acts after lateral bud formation to inhibit lateral bud growth in *Arabidopsis*. Plant Physiol 121(3):839–847

Stoma S, Lucas M, Chopard J, Schaedel M, Traas J, Godin C (2008) Flux-based transport enhancement as a plausible unifying mechanism for auxin transport in meristem development. PLoS Comput Biol 4(10):e1000207

Swarup R, Péret B (2012) AUX/LAX family of auxin influx carriers — an overview. Front Plant Sci 3(225):1–11

Swarup R, Friml J, Marchant A, Ljung K, Sandberg G, Palme K, Bennett M (2001) Localization of the auxin permease AUX1 suggests two functionally distinct hormone transport pathways operate in the *Arabidopsis* root apex. Genes Dev 15(20):2648–2653

Swarup R, Kramer E, Perry P, Knox K, Leyser O, Haseloff J, Beemster G, Bhalerao R, Bennett M (2005) Root gravitropism requires lateral root cap and epidermal cells for transport and response to a mobile auxin signal. Nat Cell Biol 7(11):1057–1065

Thimann K, Skoog F (1933) Studies on the growth hormone of plants III. The inhibitory action of the growth substance on bud development. Proc Natl Acad Sci U S A 19:714–716

Townsley B, Sinha N (2012) A new development: evolving concepts in leaf ontogeny. Annu Rev Plant Biol 63(1):535–562

van Berkel K, de Boer R, Scheres B, ten Tusscher K (2013) Polar auxin transport: models and mechanisms. Development 140(11):2253–2268

van Mourik S, Kaufmann K, van Dijk A, Angenent G, Merks R, Molenaar J (2012) Simulation of organ patterning on the floral meristem using a polar auxin transport model. PLoS One 7(1):e28762

Vieten A, Vanneste S, Wisniewska J, Benková E, Benjamins R, Beeckman T, Luschnig C, Friml J (2005) Functional redundancy of PIN proteins is accompanied by auxin-dependent cross-regulation of PIN expression. Development 132(20):4521–4531

Wabnik K, Kleine-Vehn J, Balla J, Sauer M, Naramoto S, Reinöhl V, Merks R, Govaerts W, Friml J (2010) Emergence of tissue polarization from synergy of intracellular and extracellular auxin signaling. Mol Syst Biol 6:447

Weijers D, Jürgens G (2005) Auxin and embryo axis formation: the ends in sight? Curr Opin Plant Biol 8(1):32–37

Weiss T (1996) Cellular biophysics: transport, vol 1. Bradford Books, Cambridge, MA

White A (1973) Graphs, groups and surfaces. North-Holland, Amsterdam

Xu T, Wen M, Nagawa S, Fu Y, Chen J, Wu M, Perrot-Rechenmann C, Friml J, Jones A, Yang Z (2010) Cell surface- and Rho GTPase-based auxin signaling controls cellular interdigitation in *Arabidopsis*. Cell 143(1):99–110

Zažímalová E, Murphy A, Yang H, Hoyerová K, Hošek P (2010) Auxin transporters–why so many? Cold Spring Harb Perspect Biol 2(3):a001552

Zeevaart J (2008) Leaf-produced floral signals. Curr Opin Plant Biol 11(5):541–547